Exploring the use of EMImFSI ionic liquid as additive or co-solvent for room temperature sodium ion battery electrolytes

Mohamed Benchakar, Régine Naejus, Christine Damas, J. Santos-Pena

Exploring the use of EMImFSI ionic liquid as additive or co-solvent for room temperature sodium ion battery electrolytes

Mohamed Benchakar,[a,+], Régine Naéjus,[a] Christine Damas,[a] Jesús Santos-Peña[a,b,*]

[a] Laboratoire de Physico-chimie des Matériaux et des Electrolytes pour l'Energie (PCM2E), EA 6299, Université de Tours, 37200 Tours (France)

[b] Equipe de Recherche et d'Innovation en Electrochimie pour l'Energie, ICMMO, Université Paris-Sud, UMR 8182, Rue du doyen Georges Poitou, 91495 Orsay cedex (France)

[+] Present adress: Laboratoire IC2MP, UMR CNRS-Université de Poitiers 7285, 86000 Poitiers (France)

*Corresponding author: jesus.santos-pena@univ-tours.fr

ABSTRACT

Sodium ion batteries (SIB) market are limited by their gravimetric and volumetric energies and therefore, search of high voltage redox couples combined with suitable electrolytes is nowadays mandatory. Ionic liquids can bring advantageous properties to SIB, particularly from a safe point of view, but are still quite expensive. In this pioneering work, we explore the use of small amounts of 1-ethyl-3-methylimidazolium bis(fluoromethanesulfonyl)imide (EMImFSI) ionic liquid in the electrolyte formulation, either as an additive (2% in weight ratio to a binary mixture of ethylene carbonate (EC)/propylene carbonate (PC)) or as co-solvent (10% in weight ratio). Results are compared to electrolytes containing classical SIB additive fluoro-ethylenecarbonate (FEC). Physicochemical properties of the electrolytes prepared with $NaClO_4$, $NaPF_6$ and NaFSI are differently influenced by the EMImFSI additive, which contributes with ionic species to the electrolyte ionic conductivity but increases its viscosity. Extension of the sodium plating/stripping is higher for more dissociated salt in un-doped electrolytes. Introduction of EMImFSI results in the occurrence of a SEI that hinders the plating except for the 10% EMImFSI-NaFSI based electrolyte. Electrochemical cycling of a hard carbon electrode reveals that FSI^- anion, mainly coming from the added ionic liquid, can introduce new peaks in the cyclic voltammetry or new steps in the galvanostatic discharge. The products of such degradation create an interface which determines the cycling properties. The complex picture of the interplay between sodium salt anion and EMImFSI presence and amount is not completely described in this work. However, it is clear that EMImFSI introduces initially a larger polarization in the discharge/charge curves and that only added to the $NaPF_6$ system help to stabilize the coulombic efficiency and gain in capacity (+50%). EMImFSI has not beneficial effect on the $NaClO_4$-based formulations and the initial positive effect on the sodium half cells cycled in NaFSI-based

electrolytes is cancelled after 25 cycles. Microscopy examinations on cycled electrodes reveal that coulombic efficiency and thus capacity retention are associated to a protective film completely recovering the hard carbon particles without modifying the pristine shape. This is the case for electrodes tested with un-doped $NaClO_4$ and EMImFSI-$NaPF_6$ electrolytes. Our results also show that compared with EMImFSI, FEC added in 2% weight ratio content provides much better or similar electrochemical performances at a lower price.

KEYWORDS: Sodium ion batteries, additive, ionic liquids, EMImFSI, hard carbon performance, solid electrolyte interface

1. Introduction

Nowadays, sodium ion batteries (SIB) are an alternative to lithium ion batteries (LIB) due to the high cost of lithium and its forecasted penury in a few decades [1-9]. However, sodium is a heavier atom than lithium and shows a more positive redox potential. Therefore, gravimetric capacities and energies are smaller for SIB than for LIB, preventing a realistic implementation of the SIB technology at short term. Even if expensive copper collectors used in LIB can be substituted by lighter and cheaper aluminum collectors, some studies have shown that for an attractive industrial point of view, SIB energy should be increased. This increase relies on positive electrode/negative electrode couples with high voltage difference [5] combined with electrolytic media with adequate electrochemical and chemical stability. As a consequence, deep studies have been devoted to the research on electrolytes for sodium ion batteries [10-12] and some worthy reviews shed light on this aspect of the battery formulation [13-16].

As for other technologies, SIB electrolytes require solvents with wide range of liquid temperature, high value of dielectric constant ε_r, low desolvatation energy, low viscosity, chemical stability against electrode material, wide electrochemical window (EW) and ability to build stable and suitable solid electrolyte interface [2-4,6,10-13,15,17-24,26-29]. Cyclic and linear carbonates, especially propylene carbonate (PC), ethylene carbonate (EC), dimethyl carbonate (DMC), diethyl carbonate (DEC) [2-4,9-30,] as well esters as tetrahydrofurane (THF) [3-4,9,10,13-15,17] and glymes [3-4,9,10,13-15,17] have been proposed as solvents for electrolytes. By comparison with lithium counterparts, $NaClO_4$, $NaBF_4$ and $NaPF_6$ and more complex salts were employed [2-4,9-30]. Additives have also been a source of improvement of electrolytes for SIB. They are chosen for its ability to create a solid electrolyte interface (SEI) on the negative electrode, which passivates it and allows capacity retention upon cycling. From different studies, fluoroethylene carbonate is the most advantageous additive [2-4,9,14-15,17-19,23-27,29] although it introduces cell polarization [17,30].

Recently, ionic liquids (IL) have been proposed as alternative electrolytes for sodium ion batteries due to advantageous properties including negligible vapor pressure, non-flammability, high thermal stability, high ionic conductivity, wide operating temperature range and EW as well a large solubility of organic and inorganic compounds [9-17,31]. Low degradation of IL in a battery leads to an increased long term cycling [17]. The groups of Hagiwara [32-42], Forsythe

[43-47], Wang [48-50], Palacín [51,52], Rojo [47,53,54] and Passerini [12,55,56] have been very active in using this new kind of electrolytes. From literature, the most widely employed ILs in SIB are based on pyrrolidinium cations, especially N-methyl-N-propylpyrrolidinium (named PYR_{13}, PMP or C3mpyr) and N-methyl-N-butylpyrrolidinium (called PYR_{14}, BMP or C4mpyr) [12,28,31,34,35,37-41,43-50,52-54,56], or imidazolium cations (as 1-ethyl-3-methylimidazolium, EMIm or 1-butyl-3-methylimidazolium BMIm) [51,52,57]. Anions are basically bis(trifluoromethanesulfonyl)imide (abbreviated by TFSI, TFSA or NTf_2) or bis(fluoromethanesulfonyl)imide (abbreviated by FSI, FSA or Nf_2). Tables 1 and 2 collect several of the IL studies on both, sodium ion and sodium half cells but does not intend to be exhaustive. In addition, the low solubility of transition metals in IL accounts for an unusual stability of high voltage cathodes in these electrolytes [55].

Despite their clear interest, especially from a safe point of view, IL implementation in SIB devices shows two major drawbacks from i) their high cost, not competitive with classical organic electrolytes and ii) a very high viscosity when a sodium salt is added, penalizing the device performance at fast regimes [46,51,52]. Therefore, the potential employ of IL not as sole solvent for the electrolyte but as a co-solvent, or even as additive for more fluidic solvents, is questioned. In this sense, two important reports by Forsyth et al. [46] and Palacín et al. [52] are devoted to the use of mixtures of IL (PYR_{13}FSI [46], PYR_{13}TFSI, EMImTFSI, BMImTFSI [52]) with classical organic solvents. From both, it is concluded that IL added in a small content to, for instance, EC, ensures electrode safety improvement but does not affect positively the electrode performance.

Table 1. Deep eutectic and pyridinium based IL applied in SIB studies. AC= activated carbon.

Ionic liquid	Salt, concentration	System	T(K)	Ref
NaFSI-KFSI	Molar ratio NaFSI/KFSI = 0.56/0.44	$Na/NaCrO_2$	353	32,42
		Na/Sn	363	33,42
$PYR_{13}FSI$	NaFSI 2/8	$Na/NaCrO_2$	293-363	34,37,39,42
		$HC/NaCrO_2$	283-363	40,42
		$Na/C\text{-}Na_2Ti_3O_7$	363	41,42
	NaFSI 0-60% mole ratio	-	Wide	38
	NaFSI 0-0.5 molar fraction	Na/Na	298	45
	NaFSI(> 0.5 molar fraction)	Na/HC	363	35
	NaFSI (55 mol% Na) + 30% EC	$Na/Na_3V_2(PO_4)_3$	298	46
	NaFSI: PYR13FSI (2:8 molar)	Na/Al, Na/ $NaFe_{0.4}Ni_{0.3}Ti_{0.3}O_2$	328	54
	NaFSI 1M	Na/HC, $Na/Na_{0.44}MnO_2$, $Na/NaFePO_4$, $HC/Na_{0.44}MnO_2$	298	50
	NaTFSI 0.25-1.35 $mol \cdot kg^{-1}$	Ag/Ni	298	44
$PYR_{14}FSI$	NaTFSI 0.45M	$Na/Na_{0.45}Ni_{0.22}Co_{0.11}Mn_{0.66}O_2$	293	55

$PYR_{13}TFSI$	NaTFSI 0.8M	Na/Al	283-313	52
$PYR_{14}TFSI$	NaTFSI 0.1-0.5M	Na/Ni	298-343	43
	NaTFSI 0-0.2 molar fraction	-	293-363	31
	NaTFSI 1M	Na/ortho-$Na_{0.44}MnO_2$	298	49
	NaTFSI 0.2M	Na/P2-$Na_{0.6}Ni_{0.22}Fe_{0.11}Mn_{0.66}O_2$, Na/Sb-C, full cell	298	56
	NaTFSI 0.3M	AC/$Na_3V_2(PO_4)_3$, AC/$Na_{0.67}Mn_{0.89}Mg_{0.11}O_2$	313	77
	$NaClO_4$ 1M, $NaPF_6$ 1M, $NaBF_4$ 1M, $NaN(CN)_2$ 1M	$NaFePO_4$	348	48
$PYR_{H4}TFSI$	NaTFSI 1M	AC/$Na_3V_2(PO_4)_3$, AC/$Na_{0.67}Mn_{0.89}Mg_{0.11}O_2$	313	77

Table 2. Selected Imidazolium based IL for SIB and LIB studies. EMIm = 1-ethyl-3-methylimidazolium, BMIm=1-butyl-3-methylimidazolium.

Ionic liquid	Salt or co-solvent	System	T(K)	Conductivity ($mS \cdot cm^{-1}$)	Viscosity (cP)	Density ($g \cdot cm^{-3}$)	Ref
EMImTFSI	NaTFSI 0.3-0.4M	Na/HC	303	3.9-5.3	38.94-59.37	1.53-1.56	51
BMImTFSI	NaTFSI 0.8 M, EC,PC	Na/HC	303	3.5-10	57.45-81.25	1.37-1.48	51,52
EMImFSI	NaFSI (0<x<0.5)	Na/Cu, Na/Al	298	5.4	78	1.561	36
$EMImBF_4$	$NaBF_4$ 0.1-0.75M	Na/Pt	303	11.8-14.3	-	-	57
EMImFSI	LiFSI 1.2M	Li/Si	r.t.	-	-	-	59
	LiFSI 1M	Li/Ni-Sn-Si-Al-C composite	298	10.60	32.73	1.495	61
	LiTFSI 0.8M	Li/Graphite	r.t.	-	-	-	62

In this work, we formulated nine electrolytes based on 1M solutions of $NaClO_4$, $NaPF_6$, and NaFSI salts in EC/PC/EMImFSI mixtures with a weight ratio 50/50/0, 49/49/2 and 45/45/10. Choice of EC/PC as baseline electrolyte comes from different results showing a wide electrochemical widow, reversible Na plating/stripping, sodium storage in HC with high coulombic efficiency and suitable thermal safety and stable SEI [9-17,21,26,52]. EMImFSI was selected as IL because its high cost has limited the literature for SIB purposes [36]. Unlike, FSI^- anion has been studied widely in SIB [28,32-42,46,50,53-55] and creates a SEI in LIB and SIB able to capture SO_2 derived from its degradation [28,58-60]. Thus, the LiFSI/EMImFSI or LiTFSI/EMImFSI combinations are known to show advantageous cycling properties for LIB negative electrodes as silicon [59], silicon-based composites [61] and graphite [62]. In addition, FSI^- anion stabilizes the aluminum collector [34,58]. Finally, the mixtures of EMImFSI/organic solvent have not been exhaustively studied earlier, at the best of our knowledge.

After physicochemical characterization of the nine electrolytes prepared at 298K, sodium plating/stripping from the electrolytes is discussed as well the electrochemical performance of hard carbon (HC) in sodium half-cells by using cyclic voltammetry and galvanostatic titration. The results are compared with those obtained with classic FEC additive, added in a 2% weight ratio to the baseline electrolyte [25,26]. We present here relevant information about the role of EMImFSI on increasing or decreasing the hard carbon negative electrode performance depending on its content in a ternary solvent mixture and on the sodium salt anion. Improvement in hard carbon electrochemical performance is limited to formulations containing $NaPF_6$, but can be as high as a gain in a 50% of capacity. In the case of NaFSI, the positive influence of EMImFSI as co-solvent is cancelled after 25 cycles. For the $NaClO_4$-based electrolytes, EMImFSI addition is not beneficial. The different behavior for each electrolyte formulation is related mainly to the SEI formed onto the electrode hard carbon particles. We show that, except for the EMImFSI-NaFSI-based electrolytes, the best electrochemical characteristics correspond to stable SEI recovering the hard carbon particles. This corresponds to electrodes cycled in un-doped $NaClO_4$ or EMImFSI-doped $NaPF_6$ electrolytes. Finally we demonstrate that EMImFSI is only competitive against FEC in the latter case, the EMImFSI-based electrolytes providing stable capacities close to 150 $mAh \cdot g^{-1}$.

2. Experimental.

2.1. Preparation of hard carbon

Hard carbon was prepared by treating a few grams of cellulose (*Aldrich,* pure) in an oven at 453 K for 12h and subsequently heating at 1173 K under an argon atmosphere for 8 h.

2.2. Physicochemical characterizations

Powdered hard carbon was analyzed by X-rays diffraction (XRD) with a Phillips X'PERT MPD diffractometer equipped with a Cu-Kα source instrument in the 5-70° 2θ range. Scanning electron micrography (SEM) images of the pristine hard carbon and the electrodes were obtained with a Champ Field Zeiss Ultra Plus Microscope working at 3 kV. Electrodes were observed by SEM after washing three times in the glovebox with 1 mL portions of DMC. Raman spectra were collected in the 900-1800 cm^{-1} Raman shift range through a LABRAM HR Evolution by Horiba. N_2 adsorption at 77 K and CO_2 sorption at 273 K were conducted in a Quadrasorb (Quantachrome, USA). Prior to the measurements, the samples were outgassed at 393 K for 12 h under vacuum. The specific surface area was determined from the N_2 adsorption isotherm using the Brunauer–Emmett–Teller (BET) equation. The micropores volume was determined by the non-local density functional theory (NLDFT) method with a slit-shaped pore model applied to the N_2 adsorption data.

2.3. Preparation of the electrode mixture

Electrode mixture was prepared by mixing the hard carbon, sodium carboxy-methylcellulose, NaCMC (*Aldrich*, pure) as a binder and Super P carbon black (*Timcal*) as a conductive additive. Firstly, NaCMC is dissolved in 0.7 mL of deionized water. Then, carbons are added to the solution, respecting an 80/10/10 w/w/w ratio of HC/Super P/NaCMC. After stirring for 2 h, the obtained slurry is casted onto 0.05 mm thick aluminium foil (*Goodfellows*, 98%) and dried at 338 K in air overnight. Disks of ϕ=10 mm were subsequently cut to constitute the working electrodes.

2.4. Preparation of the electrolytes

Electrolytic solutions were prepared and stored in an M-Braun glove box containing an argon atmosphere, with oxygen and water contents below 10 ppm and 0.1 ppm, respectively. Ethylene carbonate (*Sigma Aldrich,99%*) and propylene carbonate (*Sigma Aldrich,99.7%*) were dried over molecular sieve (*Chem.Genes*) for at least 24 hours before the preparations. EMImFSI (*Solvionic,*99.9%,) was used as received. The solvent mixtures were prepared by weighing the different components according a weight ratio 50/50/0, 49/49/2 and 45/45/10 (EC/PC/EMImFSI). Then, the salt was added to such mixtures to give 1M solutions that are stored at the glove box. Sodium salts were $NaClO_4$ (*Fluorochem*, 98%), $NaPF_6$ (*Fluorochem*, 98%) and NaFSI (S*olvionic,* 99.7%). Water content in the resulting solutions was checked through the Karl Fischer technique, being found to be below 50 ppm. All the preparations were carried out at 293K.

2.5. Electrochemical tests

All the tests were carried out at least three times and monitored either in MPEG2 or VMP3 Biologic apparatus. The cells were built in the MBraun glove box. Sodium plating/stripping is conducted through cyclic voltammetry (CV) on two electrodes *swagelock* cells with aluminium foil disk (ϕ=10 mm) as working electrode and sodium (*Sigma Aldrich,* 99.9%) as counter and reference electrode. Cercles (ϕ=12 mm) of Whatman GF/A separator were imbibed with 180 µL of the electrolyte. Imposed voltage limits are -0.2 V and 0.5 V vs Na/Na^+ and voltage steps were 50 $\mu V \cdot s^{-1}$.

CV and galvanostatic tests were conducted on two electrode *swagelock* cells with HC-based electrode as working electrode and sodium as counter and reference electrode. CV was carried out in the 3 mV-1.5 V vs Na/Na^+ voltage limits with voltage steps of 50 μVs^{-1}. Then, a constant current of 20 $mA \cdot g^{-1}$ (per gram of hard carbon) was applied on the electrode for the first five galvanostatic tests, continued by cycling at 20 $mA \cdot g^{-1}$. Galvanostatic cycling was conducted in the same voltage limits used for CV. Desodiation capacity discussion is preferentially proposed in this work. All the electrochemical tests were conducted at 293 K.

3. Results and discussion

3.1. Hard carbon material characterization

XRD pattern corresponding to the hard carbon electrode contains two peaks associated to the [002] and [100] plans located at 2θ= 23.07 and 43.71°. From the XRD results, L_c and L_a were estimated to be 0.8 nm and 4.92 nm, respectively. Raman spectrum features D (1342.5 cm^{-1}) and G (1598.5 cm^{-1}) bands yielding a value of L equal to 6.1 nm. SEM micrographs indicate that the particles are smooth particle conglomerates. Hard carbon has a S_{BET} of 508 $m^2 \cdot g^{-1}$ and a micropore volume of 0.21 $cm^3 \cdot g^{-1}$.

3.2. Physicochemical properties of the electrolytes prepared

Table III collects some of the physicochemical parameters (viscosity (η), conductivity (σ), density (ρ)) of the nine electrolytes prepared in this work in addition to those containing 2% of FEC at 298 K. Conductivity values in absence of EMImFSI agree with reported values for EC-based mixtures with PC [10]. Indeed, addition of EMImFSI, more viscous (24.5 $mPa \cdot s^{-1}$) than the EC/PC mixture, results in an increase of the EC/PC/EMImFSI viscosity with increasing amount of EMImFSI.

Another important parameter is ionic conductivity measured at 298 K. Due to the ionicity of EMImFSI, a larger content of EMImFSI in the EC/PC/EMImFSI mixture enhances the intrinsic conductivity of the electrolytic mixture. It is noteworthy that NaFSI-based solutions ionic conductivities are larger compared with the $NaClO_4$ and $NaPF_6$-based electrolytes. Addition of EMImFSI in a 10% content, provides ionic conductivities close to 10 $mS \cdot cm^{-1}$, which correspond to an increase of 23-39% from un-doped EC/PC mixture and are close to that of that of the r.t. working electrolyte 0.1M $NaBF_4$ in $EMImBF_4$ [57]. Therefore, addition of EMImFSI is not penalizing the conductive properties of the electrolyte. Besides, one can observe that due to the fact that PF_6^- anion is less polarizable than ClO_4^- anion, the $NaPF_6$-based electrolytes are in general more conductive [10,11].

Table 3. Physicochemical parameters (conductivity, viscosity, density) of the electrolytes prepared at 293K and adjustable parameters of VTF equation for viscosity and conductivity.

Electrolyte salt	Additive	% w/w	σ ($mS \cdot cm^{-1}$)	η ($mPa \cdot s^{-1}$)	ρ ($g \cdot cm^{-3}$)	ln σ_0	E_σ ($kJ.mol^{-1}$)	$T_{0,\sigma}$ (K)	-ln η_0	E_η ($kJ.mol^{-1}$)	$T_{0,\eta}$ (K)
$NaClO_4$		0	7.57	6.27	1.33	5.24	3.70	160	1.58	3.51	174
	EMImFSI	2	7.86	6.31	1.33	5.04	3.19	169	1.28	2.88	187
		10	10.60	7.24	1.35	5.98	4.83	138	1.14	3.00	182
	FEC	2	8.66	6.25	1.33	5.04	3.03	172	1.55	3.46	175
$NaPF_6$		0	7.92	6.04	1.35	4.16	1.42	216	1.51	3.35	176
	EMImFSI	2	8.29	6.16	1.35	4.27	1.50	214	1.47	3.28	178
		10	9.77	6.55	1.35	4.67	1.84	205	1.54	3.47	176
	FEC	2	7.97	6.03	1.35	4.63	2.25	192	1.54	3.41	175
NaFSI		0	8.54	5.80	1.34	5.44	3.99	153	1.47	3.30	175
	EMImFSI	2	8.33	5.94	1.36	6.09	5.60	129	1.44	3.24	177
		10	10.78	6.48	1.36	5.80	4.24	150	1.16	2.72	190
	FEC	2	8.75	5.80	1.34	5.87	4.87	141	1.47	3.30	175

The variations of ln(σ) and ln (η) with the inverse of temperature T are shown on Figures 1, 2 and 3 respectively for the electrolytic solutions 1M NaX (X = ClO_4, FSI, PF_6) in EC:PC. All the ln(σ) vs. 1/T plots have a curved profile and cannot be correlated by the Arrhenius equation. Thus, the ionic transport process involving intermolecular hopping described by the Arrhenius equation is not valid for such systems. We have then applied another model of ion transport involving the mobility of the solvent molecules and depending on the free volume of the solvent, described by the Vogel-Tamman-Fulcher (VTF) equation [63-65]:

$$\sigma = \sigma_0.\exp(-E_\sigma/(T-T_0)) \quad \textbf{[Eq. 1]}$$

where σ_0, E_σ and T_0 are adjustable parameters: σ_0 is generally considered as the number of charge carriers in the electrolyte system, E_σ is often considered as a pseudo-activation energy for ion transport and T_0 corresponds to the temperature at which ionic conductivity disappears. This temperature can be related to the glass transition temperature T_g value (determined from DSC analysis) whose value is in the 293-323 K range above T_0 or around 1.3 T_0 [66]. The conductivity plots [Figures 1b, 2b and 3b] correlate with a value of R^2 comprised between 0.997 and 1.000. The VTF model can also be applied to the viscosity plots [Figures 1d, 2d and 3d] following equation 2 analogous to equation 1

$$\eta = \eta_0.\exp(E_\eta/(T-T_0)) \quad \textbf{[Eq. 2]}$$

where η_0 and E_η represents the viscosity at the high temperature limit (as $T \rightarrow \infty$, it corresponds to the viscosity of the system in vapor state) and the pseudo-activation energy for the fluidity $1/\eta$, respectively. The fits yield excellent R^2 values ranging between 0.999 and 1.000. The parameters issued from the conductivity and viscosity fittings are gathered in Table 3.

In the case of viscosity results, T_0 and E_η values are similar for any electrolyte formulation, lying in the range 174-190 K and 2.7-3.5 $kJ \cdot mol^{-1}$, respectively. Therefore, EMImFSI or FEC additive or NaX (X=ClO_4, PF_6, FSI) salt have quite similar effects on the thermal viscosity behavior. Much difference is noticed in the salt or the additive impact on the thermal conductivity behavior. Given that T_0 and E_σ vary inversely, the following discussion will focus on E_σ values.

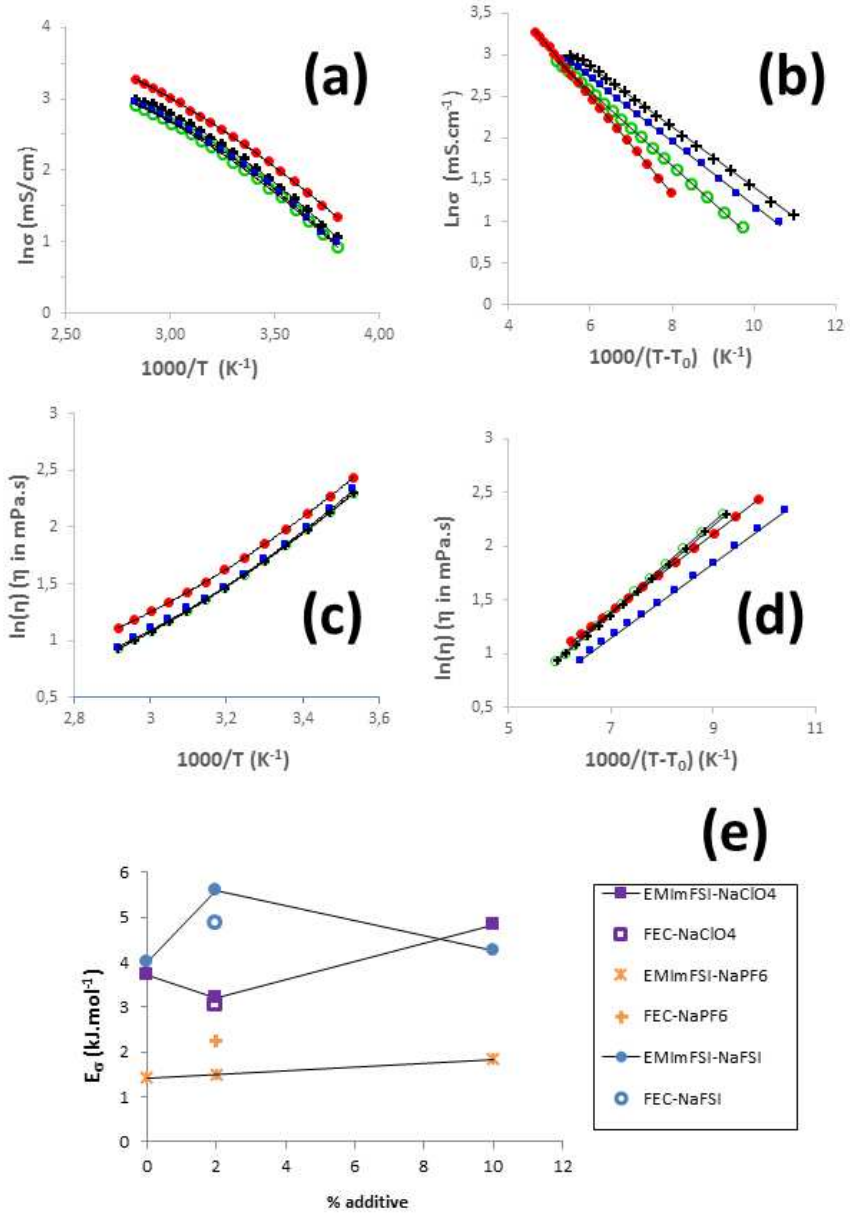

Figure 1 : Variations of ln(σ) as a function of 1/T (a) and 1000/(T-T_0) (b) and ln(η) as a function of 1/T (c) and 1000/(T-T_0) (d) for 1 M $NaClO_4$ solutions in EC:PC without additive (○), with 2% FEC (+),2% EMImFSI (●) and 10% EMImFSI (■). (e) Effect of additives content on the activation energy of the conductivity.

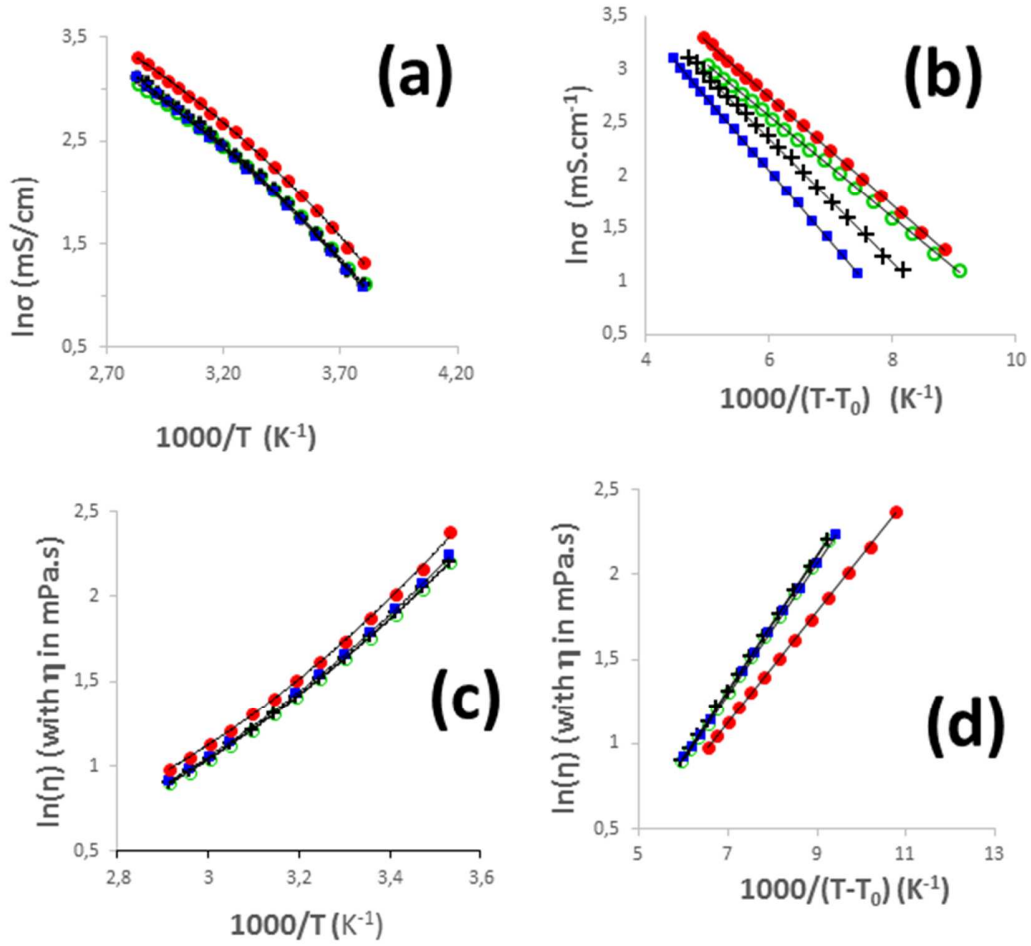

Figure 2 : Variations of ln(σ) as a function of 1/T (a) and 1000/(T-T_0) (b) and of ln(η) as a function of 1/T (c) and 1000/(T-T_0) (d) for 1 M NaFSI solutions in EC:PC without additive (○), with 2% FEC (+),2% EMImFSI (●) and 10% EMImFSI (■).

When comparing the E_σ values of the three systems without additive, such associated to $NaPF_6$ are the lowest ones, whereas those of $NaClO_4$ and NaFSI are of the same order of magnitude. The increase of σ with T is, therefore, facilitated with $NaClO_4$ or NaFSI. Such a behavior agrees with some previous results about NaFSI or $NaPF_6$ in EC:PC [67,68] or about donor number (DN) of anions [69]. At the best of our knowledge, $NaClO_4$ does not generate contact ion-pairs in PC [70]. However, Raman spectroscopy has shown that the content of contact ion-pairs or aggregates is around 12% in a 1M NaFSI solution in EC:PC [67]. Moreover, $NaPF_6$ in EC:PC

exhibits a dissociation degree as weak as 0.34 at 0.7 M [68]. So the weak ability of $NaPF_6$ to dissociate in EC:PC may inhibit the effect of the temperature on the conductivity increase. Such observations can also be correlated to the DN values of the anions which are an estimation of the strength of the interactions between the anions and other dissolved cationic species. The values are -6.2 and 7.6 kcal.mol^{-1} for X=PF_6 and ClO_4 respectively. A value of 13.2 kcal·mol^{-1} is estimated for FSI taking into account a value of 11.2 kcal·mol^{-1} found for TFSI and that DN decreases 1 kcal·mol^{-1} per added CF_2 group [69]. Hence, PF_6^- is seemingly the weakest donor anion of the present series.

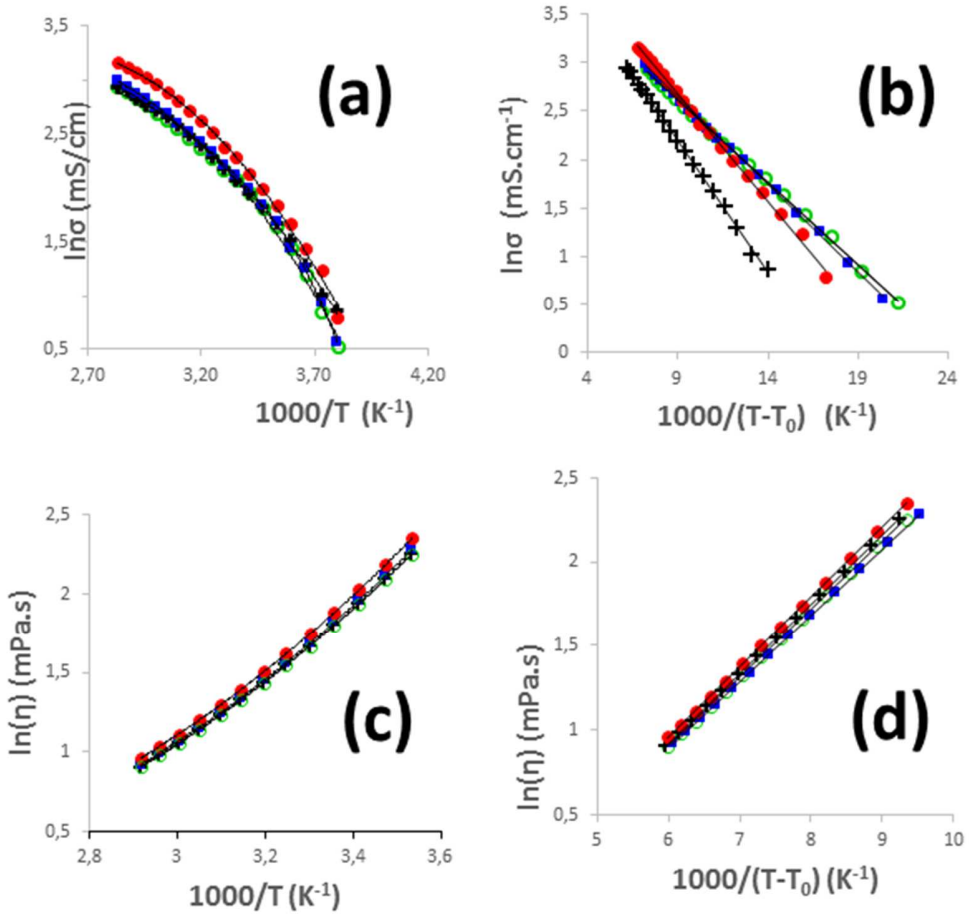

Figure 3 : Variations of ln(σ) as a function of 1/T (a) and 1000/(T-T_0) (b) and of ln(η) as a function of 1/T (c) and 1000/(T-T_0) (d) for 1 M $NaPF_6$ solutions in EC:PC without additive (○), with 2% FEC (+),2% EMImFSI (●) and 10% EMImFSI (■).

Upon addition of EMImFSI at 2% and 10%, the representation of E_σ vs. EMImFSI content (see Figure 1e) show an extremum for X = FSI or ClO_4, whereas for X = PF_6, this energy increases monotonously with the additive content. The extremum can be associated to two antagonistic effects: (i) the addition of ionic species which should facilitate the σ vs. T increase and (ii) the enhancement of the viscosity due to the addition of an ionic liquid type species which should inhibit the σ vs. T effect. Whereas the first effect rules the FSI– and PF_6–based electrolytes behavior, unlike to the case of X=ClO_4, governed by the second one. Finally, the addition of neutral and more fluid FEC at 2% w/w (as for EMImFSI) influences in a different extent the E_σ values for X=ClO_4, FSI and PF_6. The non-ionic character of FEC probably compensates its low viscosity thus leading to results quite similar to those of EMImFSI at the same content. The differences observed are therefore attributed to the sodium salt structure in solution.

3.3. Sodium plating/stripping in the electrolytic media prepared

In order to set the potential use of any electrolyte in SIB, the reversibility of the sodium plating reaction defined by

$$Na^+ + e^- \rightarrow Na \quad [1]$$

has been checked [20,32,34,36,42-44,46,52]. Figure 4 shows the plating/stripping of sodium onto an aluminum collector by means of CV. The curves corresponding to 2% EMImFSI-based electrolytes are shown in Figure S1. Hagiwara [32,34,36,42] and Forsyth [43,44,46] groups indicated that several electrolytes with the FSI^- anion (for instance, KFSI/NaFSI deep eutectics) allow such process. This contrasts with the results of Palacín et al. [52] claiming that unlike to FSI^-, pure TFSI-based ionic liquids or NaTFSI solution in PC do not allow Na plating/stripping process. They explained this feature on the basis of the formation of a film not permeable to sodium ions or to the decomposition of $TFSI^-$ anion or organic cations hindering the whole process. Sodium plating/stripping can be however obtained with NaTFSI dissolved in EC/PC [71].

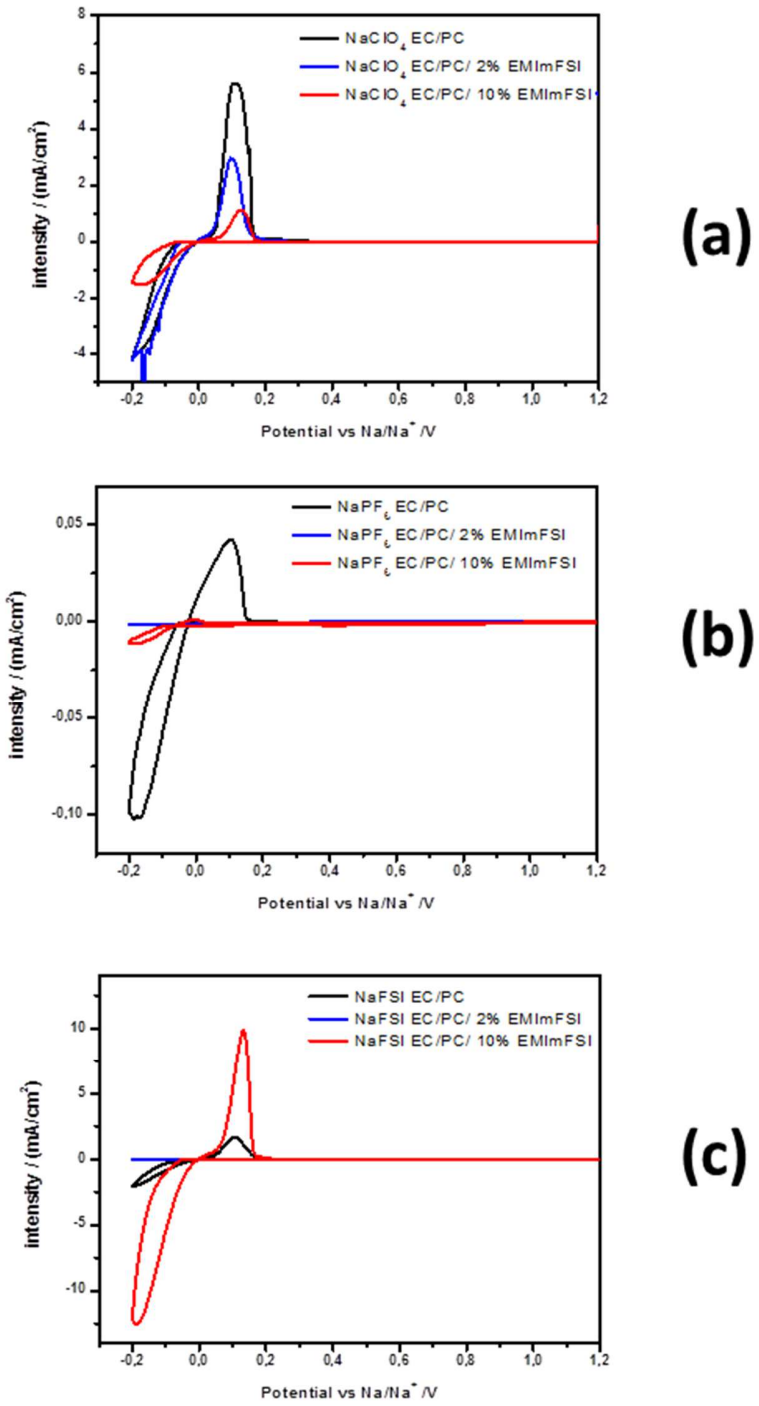

Figure 4 : Sodium plating/stripping in Na/NaX 1M/Al half cells with X= (a) ClO_4, (b) PF_6 and (c) FSI in EMImFSI/EC/PC ternary mixtures. Sweep rate: 50 $\mu V \cdot s^{-1}$. Upper voltage limits: -0.2V – 0.5V vs Na/Na^+.

Table 4 shows the onset values for plating and stripping as well the coulombic efficiency (CE) for the first cycle. In un-doped electrolytes, CEs follow the trend $NaClO_4$ ~NaFSI >> $NaPF_6$ with a larger sodium plating for $NaClO_4$. These features agree with the dissociation level of NaX in the EC/PC mixture. In the case of $NaClO_4$, onset values (approx. -50 mV vs Na/Na^+) are slightly affected by the presence of EMImFSI. Nevertheless, EMImFSI decreases both the extent of the plating and the CE (-10%).

Table 4. Sodium plating/stripping parameters in Na/Al half cells with different electrolytes prepared in this work.

Electrolyte salt	% Additive	Plating onset potential (mV)	Stripping onset potential (mV)	Coulombic efficiency (%)
$NaClO_4$	0	-52	0	80
	2% EMImFSI	-47	-6	70
	10% EMImFSI	-62	0	72
	2% FEC	-40	0	76
$NaPF_6$	0% EMImFSI	-79	-52	20
	2% EMImFSI	-169	-	n.a.
	10% EMImFSI	-85	-62	30
	2% FEC	-95	-43	46
NaFSI	0	-48	0	80
	2% EMImFSI	-130	-51	n.a.
	10% EMImFSI	-48	0	79

2% EMImFSI concentration in the $NaPF_6$- and NaFSI-based electrolyte causes very small sodium deposition and null or almost null stripping (Figure S1). Sodium plating is largely hindered, occurring at -169 mV and -130 mV for $NaPF_6$ and NaFSI-based electrolytes, respectively, which correspond to shifts of -90 mV and -82 mV compared to the respective un-doped electrolytes. These effects are not associated to the electrolytes viscosity [13] as all show similar viscosity values. For such electrolytes, broad and intense peaks are observed at 0.02-0.2V and 0.63V vs Na/Na^+ for $NaPF_6$ and NaFSI solutions, respectively. Unlike, 10% EMImFSI has a slight effect on plating extent and cycling efficiency of NaFSI solutions, without apparent shift of the onset values. Furthermore, plating and stripping gap are similar to that of the un-doped electrolytes.

As stated by Palacin et al. [20,52], plating/stripping results reveal a very important role of the SEI formed in any cell. Decomposition products of solvent and sodium salt modify the ability of sodium for achieving reve rsible Eq. 1. For instance, increase of reversibility and CE denotes the formation of a suitable SEI onto the aluminum collector [18] when FEC is used as additive. In this sense, the values collected in Table 4 for FEC-containing electrolytes agree with a positive or null effect of this particular additive on the reversible sodium electrodeposition.

3.4. Sodium storage in the hard carbon material

3.4.1. Sodium storage during the first CV

Sodium half cells were built with a hard carbon electrode as working electrode. Mainly, two main mechanisms have been proposed for explaining the sodium storage. Dahn's group [72] earlier proposed the *house of cards* model that considers two steps in the sodium ions storage, initially in the graphene layers of the hard carbon turbostratic domains followed by storage in defaults and microporosity. Later, Ji et al. [17,73] proposed a model more consistent with the analogous lithium insertion in graphene-base systems. Thus, sodium ions store initially in the turbostratic domains defaults, then adsorb on the micropores and finally insert into the graphene layers. The steps above described for any model correspond to two distinct features noticed in the galvanostatic discharge after an initial quick polarization: a linear voltage/composition region until 0.1V vs Na/Na^+ followed by a pseudo-plateau at such potential. At slightly lower voltages, Ji's group also pointed sodium plating. A recent review [74] proposes alternative new models for sodium ion storage.

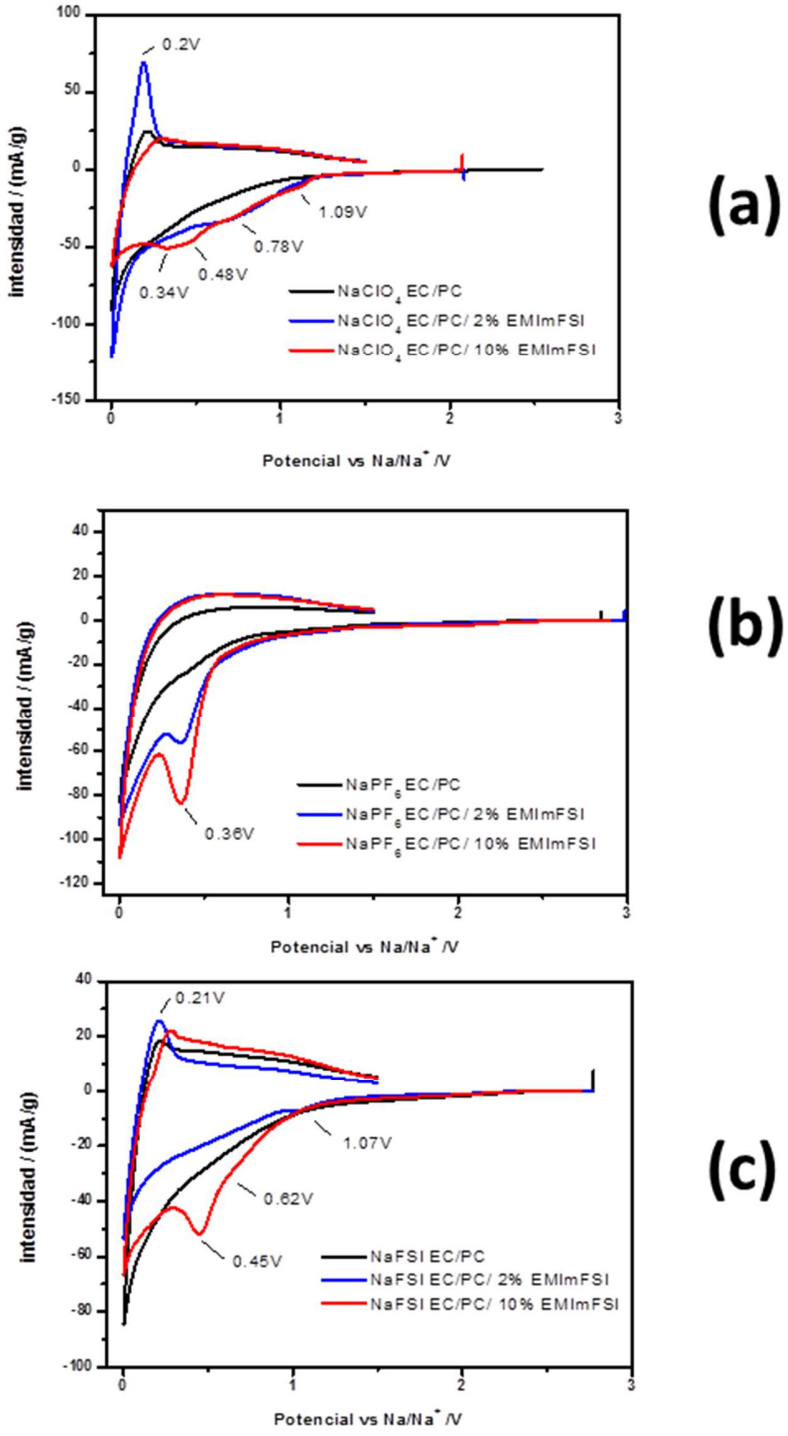

Figure 5: First CV of Na/NaX 1M/hard carbon half cells with (a) X=ClO_4,(b) X= PF_6 and (c) X=FSI in EMImFSI/EC/PC ternary mixtures. Sweep rate: 50 $\mu V \cdot s^{-1}$. Voltage limits: 3 mV – 1.5V vs Na/Na^+.

First cyclic voltammetries under 50 $\mu V \cdot s^{-1}$ corresponding to the nine electrolytes of this study are shown in Figure 5. CV was performed at such very low scan rate, in order to develop the SEI. The morphology, composition and suitability of this interface for electrochemical cycling will be described in section 3.5.

In the CV curves, the three steps above mentioned for sodium storage are noticed. Thus, one can observe an almost horizontal line from OCV to 0.1V vs Na/Na^+, followed by a sloping region until 0.01V vs Na/Na^+ and finally an incomplete intense peak, very close to 0V vs Na/Na^+. The most important feature during the charge of the electrode is a peak observed at 0.2V vs Na/Na^+. This well resolved peak is associated to sodium ions desorption from the hard carbon microporosity, according to Dahn's group [72], or to the desinsertion of sodium ions from the interlayered space separating the graphene layers, according to Ji's group [73]. Stripping of sodium should also be considered as the presence of a porous electrode (hard carbon) instead of the planar aluminum foil modifies the plating/stripping potentials.

The effect of EMImFSI content on the electrolyte containing $NaClO_4$ is now examined (Figure 5a). For the un-doped electrolyte, the electrode provides a CV typical of hard carbon electrode. Introduction of EMImFSI in a 2% w/w content enhances the electrochemical activity of the electrode (gravimetric intensities increase) but also introduce a new feature during the first discharge, a broad band develops after 1.23V vs Na/Na^+ with maxima at 1.09V and 0.6V. The same accounts for 10% w/w of EMImFSI. Thus, the band is unambiguously associated to the presence of the IL in the electrolytic mixture. For the 10% EMImFSI-based electrolyte, a duplicate peak is noticed with maxima at 0.48V and 0.34 V vs Na/Na^+**.** The occurrence of these cathodic peaks in both doped electrolytes indicates a consumption of sodium from the electrolyte in order to create the SEI. Thus, a similar chemical nature for the SEI is expected for both electrolytes, but SEI thickness should be larger for the 10% EMImFSI content. A thick SEI should hinder the sodium uptake/release from the hard carbon particles, as observed in Figure 5a.

Figure 5b shows the CV associated to the half-cell cycled in presence of $NaPF_6$-based electrolytes. In agreement with the former results of sodium plating/stripping, gravimetric capacities are very low for these half-cells. Incorporation of EMImFSI to the electrolyte leads to the occurrence of an irreversible peak in the cathodic wave (ca. 0.36V vs Na/Na^+). The same

accounts for the NaFSI-based electrolyte. Thus, in line with Figure 4c, the electroactivity of hard carbon in un-doped NaFSI–based and $NaClO_4$–based electrolytes is similar with slightly lower gravimetric intensities compared with the former one. Presence of EMImFSI in the electrolyte associates the apparition of new peaks in the cathodic wave located at 1.07V (for 2% EMIFSI and 10% EMImFSI), 0.62V and 0.42V (for 10% EMImFSI), values close to those found for 10% EMImFSI-$NaClO_4$ electrolyte.

Influence of the EMImFSI additive on the first half-cell CV is related to the formation of the solid electrolyte interface coming from the degradation of the electrolyte. Several peaks observed in the first cathodic wave are associated to the decomposition of the IL itself rather than to the sodium salt anion. Taking into account the controversy about the stability [36,58] or the instability [59] of $EMIm^+$ cation in negatively polarized or reductant surfaces, it seems more suitable the association of the new peaks to the FSI^- anion degradation, that has been earlier documented [28,58-61]. This would be consistent with FSI^- anion from the IL more associated to the $EMIm^+$ cation and available to reduce onto the negatively polarized electrode surface. Unlike, FSI^- anion coming from the salt is strongly coordinated by largely in excess EC molecules and less prone to its reduction. The suitability of the SEI thus formed and its stability will be checked in the next sections.

3.4.2. First galvanostatic cycle after one CV

Figure 6 shows the first and sixth galvanostatic cycles following the CV described in the section 3.4.1. First and sixth cycles are conducted on different regimes (20 $mA \cdot g^{-1}$ and 40 $mA \cdot g^{-1}$, respectively) in order to show the half-cell performance stability with increasing regime rate (C-rate testing). The cycling corresponding to 2% FEC-based electrolytes is collected in Figure S2.

Half-cell cycled with an EMImFSI-free $NaClO_4$-based electrolyte (Figure 6a) provided a typical voltage/composition, containing the initial voltage polarization, the sloping region at 1.0V and the pseudoplateau at the lowest voltage. The profiles are mainly maintained after discharging/charging under a faster regime. Nevertheless, a change in the polarization is noticed: 26 mV (1st cycle) and 103 mV (6th cycle).

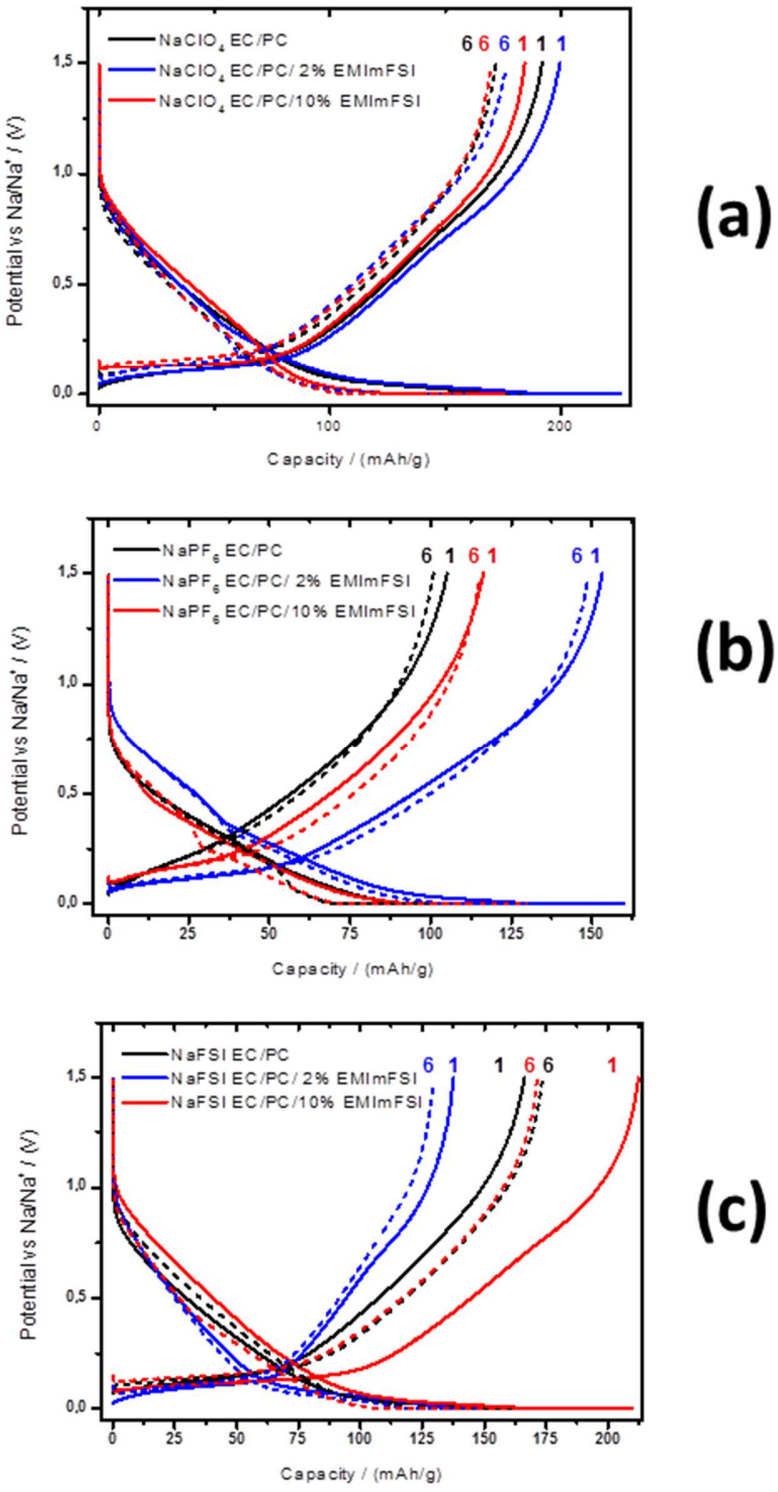

Figure 6: First sodiation/de-sodiation cycle (under 20 $mA \cdot g^{-1}$) and sixth sodiation/de-sodiation cycle (under 40 $mA \cdot g^{-1}$) of Na/NaX 1M/hard carbon half cells with (a) X=ClO_4, (b) X= PF_6 and (c) X=FSI in EMImFSI/EC/PC ternary mixtures. Voltage limits: 3 mV – 1.5V vs Na/Na^+.

Introduction of EMImFSI slightly influences the electrochemical performance of the electrode during the first six cycles, with similar profiles to those observed in absence of EMImFSI. However, polarization increases to 43 mV (for 2% EMImFSI) and 120 mV (for 10% EMImFSI) and levels off to 81 mV and 152 mV after 6 cycles for 2%EMImFSI and 10%EMIFSI respectively. A more resistive SEI has been observed when switching from EC/DEC-based to BMPTFSI-based ionic liquid electrolytic solutions containing $NaClO_4$ and $NaPF_6$ [48]. The different polarizations agree with a distinct solid interface created for every electrolyte formulation [4,24,29,30,52]. Table 5 indicates that EMImFSI-based electrolytes provide similar de-sodiation capacities and capacity retention at different current regimes. Such values are slightly lower than those observed for the classic FEC additive (Figure 7d), which turns to provide the lesser polarization. For the 6th cycle, capacity retention follows the rank 2% FEC > 10% EMImFSI > 0% EMImFSI,FEC > 2% EMImFSI. An average de-sodiation capacity of 175 $mAh \cdot g^{-1}$ is provided by the sodium half-cells operating with un-doped $NaClO_4$-based electrolyte at the 6th cycle.

Poorer performance of $NaPF_6$-based half-cells (Figure 6b) compared with $NaClO_4$-based ones is noticed during galvanostatic cycling. Thus, such devices provide 50-90 $mAh \cdot g^{-1}$ less of capacity in the first cycle. Interestingly, for $NaPF_6$, the discharge/charge profiles depend on electrolyte composition and cycle number. Thus, first cycle with 0% and 2% EMImFSI are quite similar in profile. However, the sixth discharge is severely modified for both half-cells, showing abrupt voltage decay beyond 0.17V and 0.37V vs Na/Na^+ for 0% EMImFSI and 2% EMImFSI respectively. On the opposite, the 10% EMImFSI-based cell provided a major feature in the first discharge curve (a 35 $mAh \cdot g^{-1}$ wide pseudo-plateau up to 0.37 V) that would be responsible for the profile maintenance after 5 cycles. This feature is related with EMImFSI decomposition. Regarding the polarization between sodiation and de-sodiation steps, the values are as follows: 43.8 mV, 56.7 mV and 94 mV (1st cycle for 0, 2 and 10% EMImFSI respectively) and 113 mV, 98 mV and 123 mV (6th cycle for 0, 2 and 10% EMImFSI respectively). Thus, as for $NaClO_4$-based cells, the doping with EMImFSI also increases initially the polarization although 2% EMImFSI-based cell shows the smallest polarization after cycling.

Table 5. Polarization and desodiation capacities for the sodium hard carbon half-cells (1st cycle and 6th cycle) and capacity retention with the electrolytes prepared in this work.

Electrolyte salt	% Additive	Desodiation capacity at 1th cycle (C/10) ($mAh \cdot g^{-1}$)	Polarisation (mV)	Desodiation capacity at 6th cycle (C/5) ($mAh \cdot g^{-1}$)	Polarisation (mV)	Capacity retention (%)
$NaClO_4$	0	192	23	172	100	89.58
	2% EMImFSI	200	40	176	78	88.00
	10% EMImFSI	184	117	169	149	91.85
	2% FEC	175	42	175	75	100
$NaPF_6$	0% EMImFSI	102	41	100	110	98.04
	2% EMImFSI	160	54	150	95	93.75
	10% EMImFSI	118	91	119	120	100.84
	2% FEC	136	19	135	45	99.26
NaFSI	0	166	69	179	92	107.83
	2% EMImFSI	138	22	124	99	71.74
	10% EMImFSI	214	82	171	144	80.00
	2% FEC	214	39	215	42	100.47

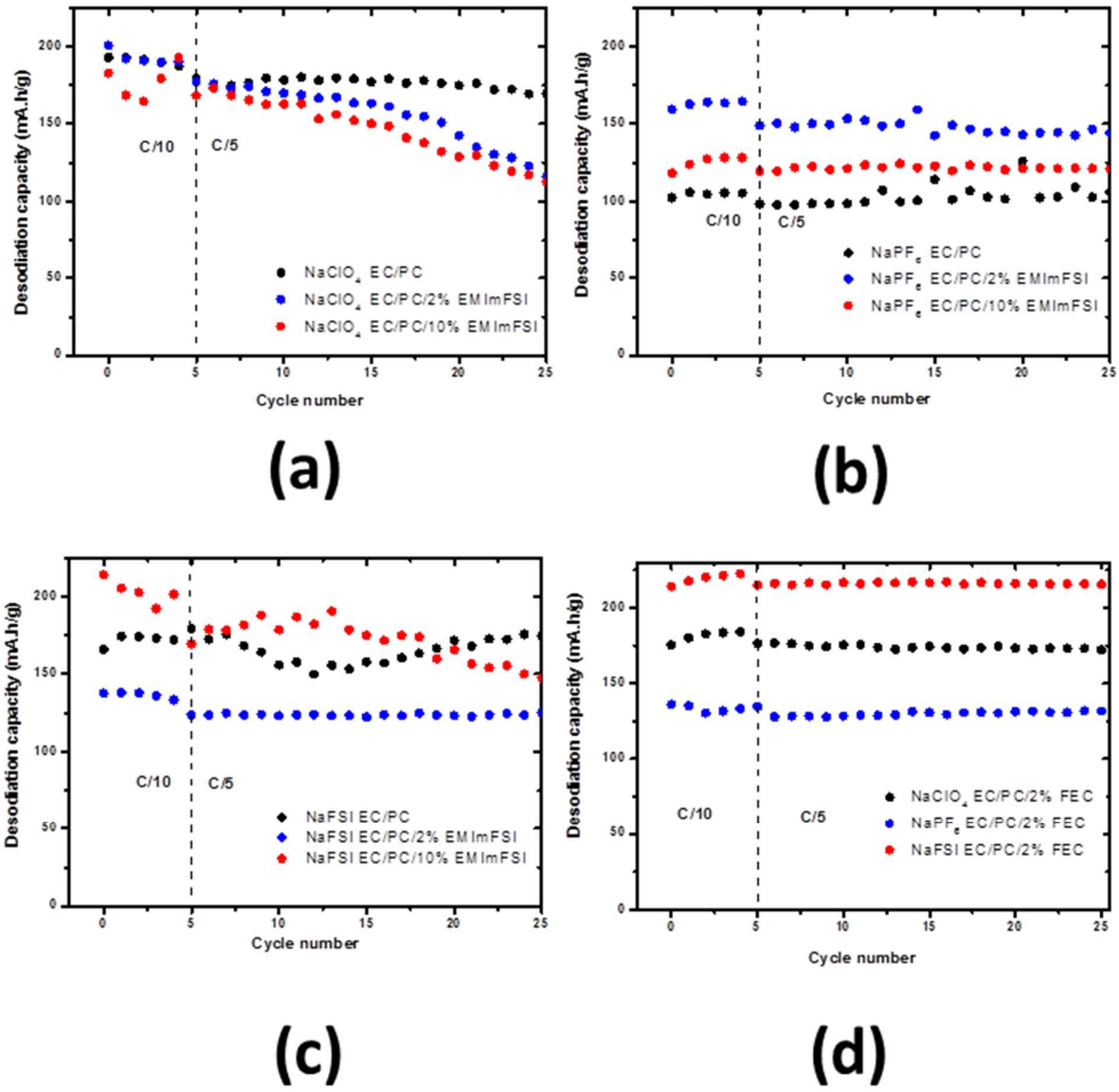

Figure 7: Evolution of the sodiation (discharge) capacity during prolonged galvanostatic cycling (5 cycles under 20 mA·g^{-1} and 20 cycles under 40 mA·g^{-1}) of Na/NaX 1M/hard carbon half cells with (a) X=ClO_4, (b) X= PF_6 and (c) X=FSI in EMImFSI/EC/PC ternary mixtures, (d) X=ClO_4, X= PF_6 and X=FSI in FEC/EC/PC ternary mixtures. Voltage limits: 3 mV – 1.5V vs Na/Na^+.

Doping the $NaPF_6$-based electrolyte with EMImFSI has a positive effect on the de-sodiation capacities (Table 5) which are increased, but as for $NaClO_4$-based electrolytes, 2%EMIFSI

corresponds to the lower capacity retention. This feature is even more noteworthy when compared with a FEC-doped electrolyte, which half-cells performed in average better (Figure 7d) and show the smaller polarization. The rank for capacity retention is 10% EMImFSI > 2% FEC > 0% EMImFSI,FEC > 2% EMImFSI. Nevertheless, the highest de-sodiation capacity was found at the 6th cycle (150 mAh·g^{-1}) and corresponds to 2%EMImFSI.

NaFSI-based sodium half-cells (Figure 6c) show similar shapes to those containing $NaClO_4$, although the capacities provided are different. Thus, for 0% and 2% EMImFSI, the half-cells furnished a lower capacity. This trend is reversed for the 10% EMImFSI-based cell that provides 25 mAh·g^{-1} more than for $NaClO_4$. Polarization of the cells does not follow a trend according to the EMImFSI content in the electrolyte (Table 5) but are higher than that found for FEC. Nevertheless, one can note that unlike its $NaClO_4$ and $NaPF_6$ counter-parts, the more stable interface corresponds to 0% EMImFSI electrolyte with only an increase in the polarization of 34%. Finally, the rank for capacity retention after six cycles is 2% FEC> 0% EMImFSI,FEC > 10% EMImFSI> 2% EMImFSI, the 2%FEC-based electrolyte providing the highest de-sodiation capacity (215 mAh·g^{-1}).

3.4.3. Prolonged cycling under galvanostatic conditions

Figure 7 shows the prolonged cycling of the sodium half-cells following the protocol one CV, five galvanostatic cycles under 20 mA·g^{-1} and twenty galvanostatic cycles under 40 mA·g^{-1}. The curves warrant several comments. First of all, for $NaClO_4$–containing electrolytes (Figure 7a), one can observe the cancellation of the initial positive impact of introducing EMImFSI in the electrolyte after ten cycles. Then, the de-sodiation capacity stabilizes close to 175 mAh·g^{-1} in the absence of EMImFSI whereas it declines for the EMImFSI-doped electrolytes. This behavior is opposite to that found when $NaPF_6$ is the sodium salt (Figure 7b). Thus, EMImFSI-doped electrolytes provide a stable capacity, 25-50 mAh·g^{-1} higher than un-doped electrolyte. Regarding the NaFSI-based electrolytes (Figure 7c), only 10% EMImFSI ensures a capacity higher than the EMImFSI-free electrolyte during at least 20 cycles.

At the 25th cycle, the rank of capacities with un-doped electrolytes is NaFSI > $NaClO_4$ >> $NaPF_6$, the highest capacity being 175 $mAh \cdot g^{-1}$. For the 2% EMImFSI, the rank is $NaPF_6$ > NaFSI > $NaClO_4$ with 144 $mAh \cdot g^{-1}$ as the highest capacity provided. Finally, for the 10% EMImFSI, the rank is NaFSI >> $NaPF_6$ > $NaClO_4$ with the highest capacity of 147 $mAh \cdot g^{-1}$. These results show the interplay role of salt anion and IL present in the electrolyte and reveal the advantageous properties of NaFSI as sodium salt for designing new SIB electrolyte formulations.

Capacity evolution on cycling must be compared with that obtained for 2% FEC-derived electrolytes (Figure 7d). After 25 cycles, stables capacities of 172, 132 and 216 $mAh \cdot g^{-1}$ are provided by $NaClO_4$-, $NaPF_6$- and NaFSI-based electrolytes, respectively. These results agree with the reported good characteristics of FEC as additive for SIB electrolytes [2-4,9,14-15,17-19,23-27,29].

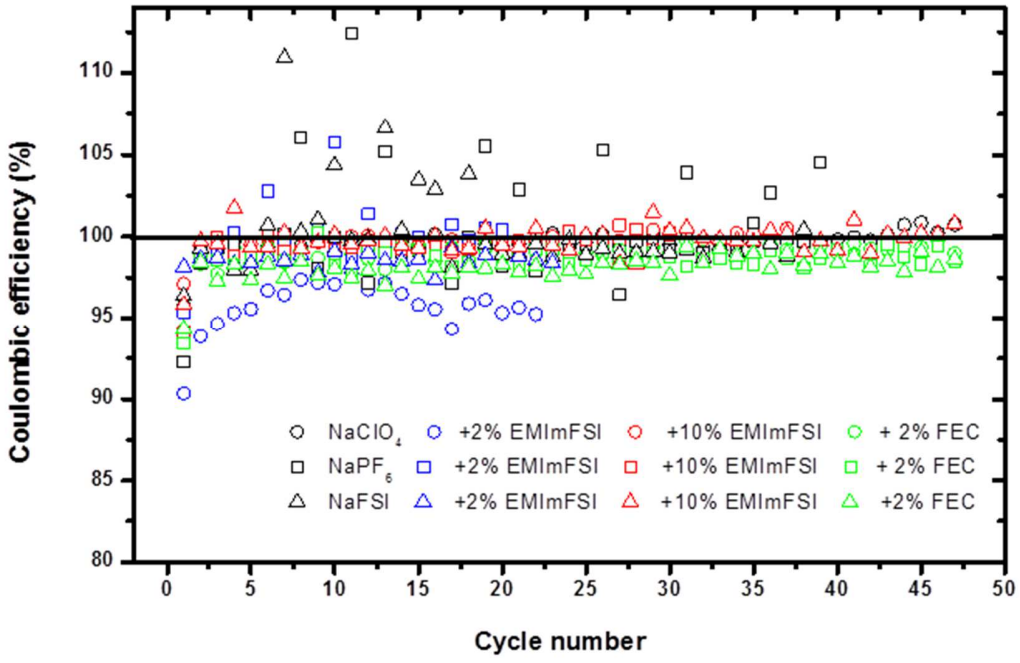

Figure 8: Evolution of the coulombic efficiency, CE, during galvanostatic cycling of Na/NaX 1M/hard carbon half cells with EMImFSI/EC/PC or FEC/EC/PC ternary mixtures. X=ClO_4, PF_6, FSI. Voltage limits: 3 mV – 1.5V vs Na/Na^+.

Disparate behavior of the nine different electrolyte formulations is also observed by examining the CE upon cycling (Figure 8) until 50 cycles for most of the electrolyte formulations. In the case of $NaClO_4$, 0% and 10% EMImFSI in the composition ensures a CE close to 100%, but only the un-doped electrolyte provides stable values of CE. For $NaPF_6$, values are random for 0% EMImFSI and 2% EMImFSI, with only 10% EMImFSI providing a stable CE close to 100%. Finally, for NaFSI-based electrolytes, it produces unstable CE values which are closest to 100% with the 10% EMImFSI composition. These observations will be reanalyzed in the section 3.5 devoted to the SEI studies. For comparison, the CE evolution on cycling for 2% FEC-based electrolytes is also shown in Figure 8. The CE provided by these formulations are stable and in the 98-99.5% range without noticeable dependence with the sodium salt [17, 25]. These advantageous CE values confirm the suitable SEI formed on the electrode particles in presence of FEC.

3.5. Solid electrolyte interface studies

The above presented results concerning polarization and cycling properties agree with a relevant role of the SEI formed between the hard carbon electrode and the electrolyte. The importance of the SEI in SIB has been formerly discussed by Komaba et al. [18]. Thus, the choice of SIB electrolytes should not be guided by their particular physicochemical parameters but to the ability to form a suitable SEI [17]. Unlike for LIB employing similar organic solvents, SEI found in SIB mainly contains inorganic layers [2,10,17,19,21,26]. SEI thickness ranges between 10 nm-30 nm depending on the electrode material [13,17,22,28].

SEI composition reflects both the salt and the solvent in the electrolyte formulation [2,4,10,11,13,15,17,20-24,26,28,29,48,52,67]. Thus, for instance, $NaClO_4$ and $NaPF_6$ decomposes to yield NaCl [19,21,26] and NaF [17,26] respectively. Organic carbonate solvents yield mainly Na_2CO_3 [2,10,15,19,75] and in lesser extent, alkylcarbonates as semicarbonates [2,10,15,18,19,26,28,76]. There is some controversy about the absence or the presence [10,17,18] of $–CH_2-$ long chained compounds, although they seem to be less present than in the lithium counter-part SEI, which justifies a more homogeneous and porous film in SIB than in LIB [17]. Additive degradation products can also participate in the SEI composition. For instance, FEC decomposes yielding NaF and Na_2CO_3 [18]. In the case of FSI-containing IL with AFSI ($A=Li^+$ or Na^+), SEI contains as common products AF and ASO_2F ($A=Li^+$, Na^+) and

trapped SO_2 [28,58-60,67] probably from the degradation of both, the IL and the alkaline salt anion.

3.5.1. SEM observations

CE values clearly indicate that the SEI is not stabilized for most of the selected electrolyte compositions. In this section we examine the cycled electrodes by SEM in order to obtain information about the SEI morphology and chemical nature.

In the $NaClO_4$-based formulations, the half-cell tested in 2%EMImFSI-containing electrolyte provided disparate CE values whereas the un-doped counter-part was quite stable. Figures 9(a,b) show the electrode after 50 galvanostatic cycles tested in un-doped electrolyte. Electrode particles are welded by a film with very few cracks. Particles with typical morphology of hard carbon are not distinguished revealing that the whole pristine electrode is buried under a film, presumably the SEI. A very different shape is shown in Figures 9(c,d) for the electrode cycled in presence of 2% EMImFSI. Indeed, the hard carbon particles are easily recognized (Figure 9c) and are recovered by nanoparticles not identifiable as carbon black present in the electrode formulation. EDS spectra (Figure 9e) indicate the presence of Na, C, O and Cl in the electrode when EMImFSI is absent. Whereas Na_2CO_3 has been proposed as the major inorganic component of the SEI, degradation of $NaClO_4$ can justify the presence of NaCl. EMImFSI addition to the electrolyte implies the occurrence of S peaks and a bigger contribution of C (Figure 9f). Cl coming from $NaClO_4$ dissociation is detected in a similar proportion. The effect of EMImFSI introduction (in 2% or 10% content) is the decomposition of FSI anion [28,58-60] that yield carbon- and sulphur-containing compounds in a powdered form. The two different features for un-doped and EMImFSI-doped electrolytes confirm the occurrence of a suitable SEI only for the first case.

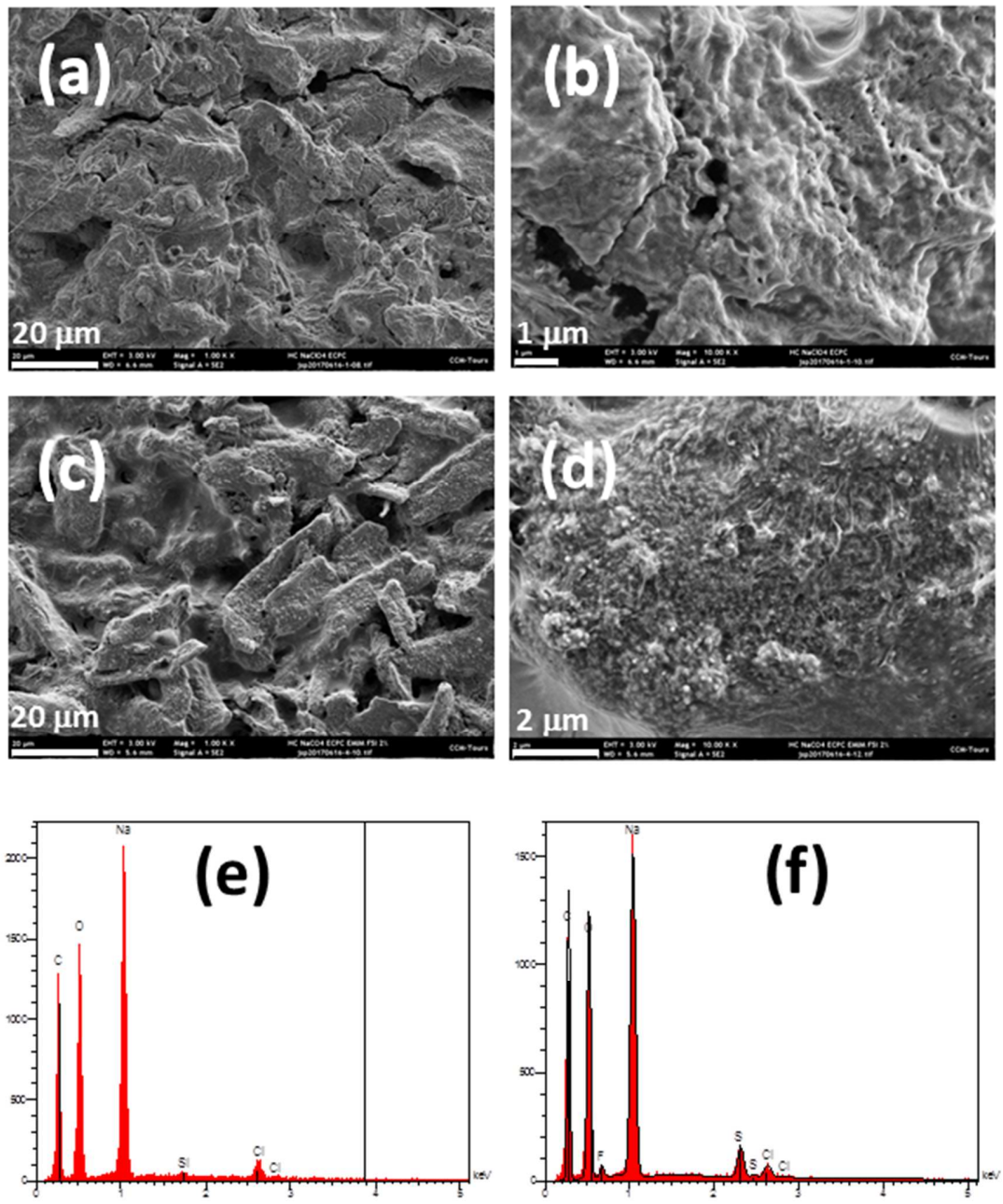

Figure 9: SEM micrographs of electrodes after 50 cycles in (a,b) 0%-EMImFSI and (c,d) 2%-EMImFSI $NaClO_4$-based electrolytes at the discharged state. (e,f) Corresponding EDS mappings.

The opposite behavior is found when $NaPF_6$ is employed as sodium salt and the electrodes are cycled for 50 times in a 0% EMImFSI (Figures 10a,b) or 10% EMImFSI (Figures 10c,d) electrolyte. Thus, for the un-doped electrolyte, the hard carbon particles are observed. When solvent is doped with EMImFSI in a 10% content, the pristine morphology of hard carbon particles is retained, but they are coated and agglomerated by a dense film which creates a protected electrode without cracks. These observations are in line with the disparate values of CE for the un-doped electrolyte and the stability of CE (and value close to 100%) for the 10% EMImFSI-doped one. EDS measurements for 0% EMImFSI (Figure 10e) indicate that the SEI contains product of the electrolyte salt and solvent, providing C, O, F, P and Na peaks presumably associated to sodium alkylcarbonates, Na_2CO_3, NaF and $Na_xPF_yO_z$ [26,28,76]. When EMImFSI was added, there are dramatic changes in the EDS spectra (Figure 10f). The system contains a larger contribution of O, F and Na. On the other hand, P and S peaks are almost undistinguishable (their potential position has however presented in the spectra for clearness). Degradation of IL FSI anion was observed for 2% EMImFSI-$NaClO_4$ electrolyte earlier, resulting in F and S peaks. However, in the current case, S peaks are almost absent. Furthermore, one can hardly hypothesize that F peaks are originated by the $NaPF_6$ degradation since a large contribution of P peaks would be expected, the only phosphorus source being $NaPF_6$. These features are consistent with a buried inorganic film onto the hard carbon particles containing $Na_xPF_yO_z$ and $NaSO_2F$ products but this statement need to be confirmed by XPS analysis.

Finally, the SEM images for the NaFSI system are collected in Figures 11a-d. CE for these systems indicated an unstable SEI during the cycling. Indeed, hard carbon particles retained their morphology after 50 cycles in un-doped and 10% EMImFSI-doped electrolytes. Several cracks in both electrodes are noticeable indicating the absence of a film coating the particles. A closer examination reveals that in the case of cycling in un-doped electrolyte (Figure 11b), the hard carbon particles are covered by randomly dispersed carbon black nanoparticles earlier present in the electrode formulation. Thus, these examinations indicate unambiguously that the washing with DMC is able to remove the protective film formed in the un-doped electrolyte. In this case, EDS gives very limited information about the chemical nature of the SEI (Figure 11e). Indeed, one can say that insoluble products contain Na, C, O and S, indicating that the FSI^- anion salt is decomposed upon cycling [67].

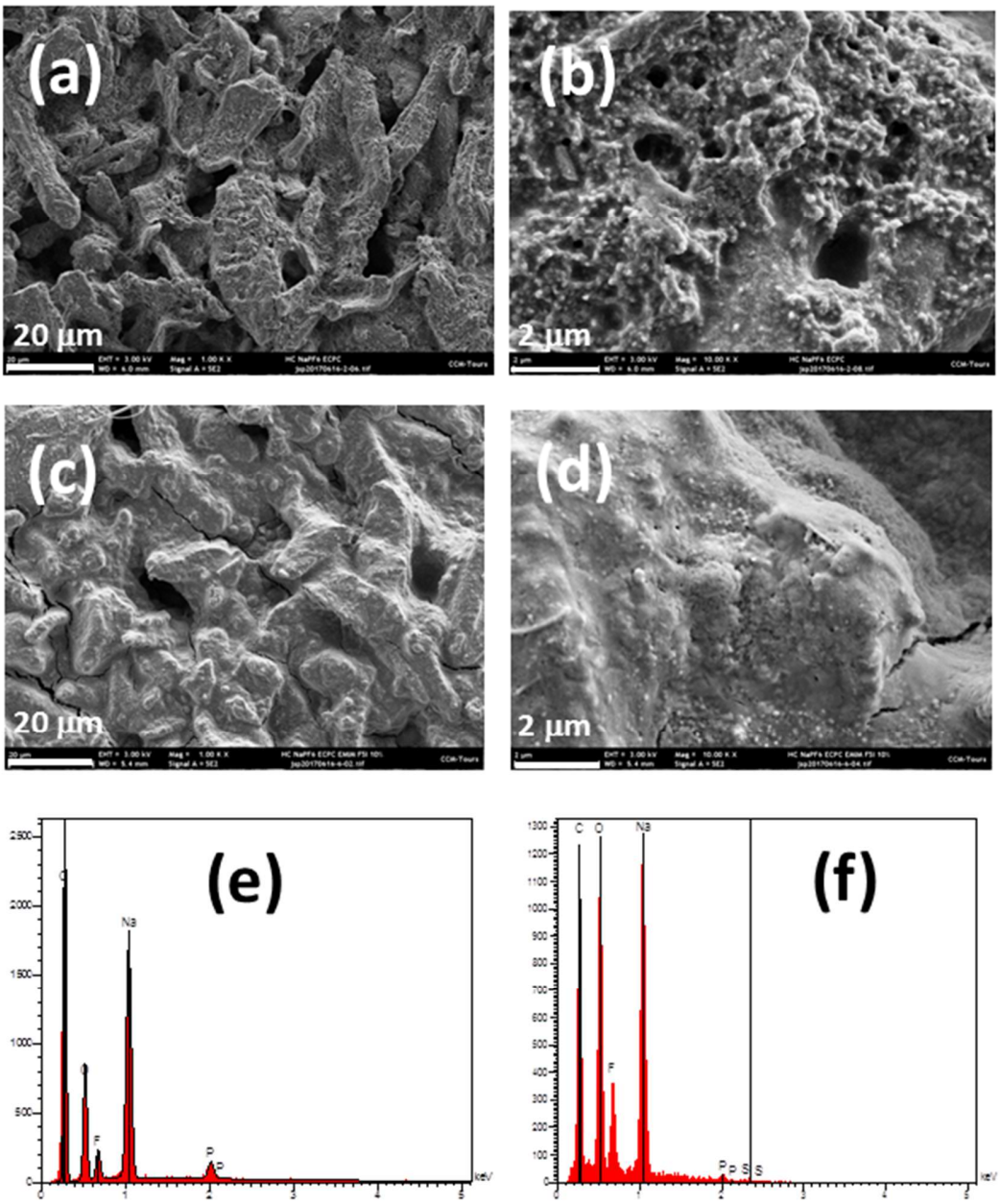

Figure 10: SEM micrographs of electrodes after 50 cycles in (a,b) 0%-EMImFSI and (c,d) 10%-EMImFSI $NaPF_6$-based electrolytes at the discharged state. (e,f) Corresponding EDS mappings.

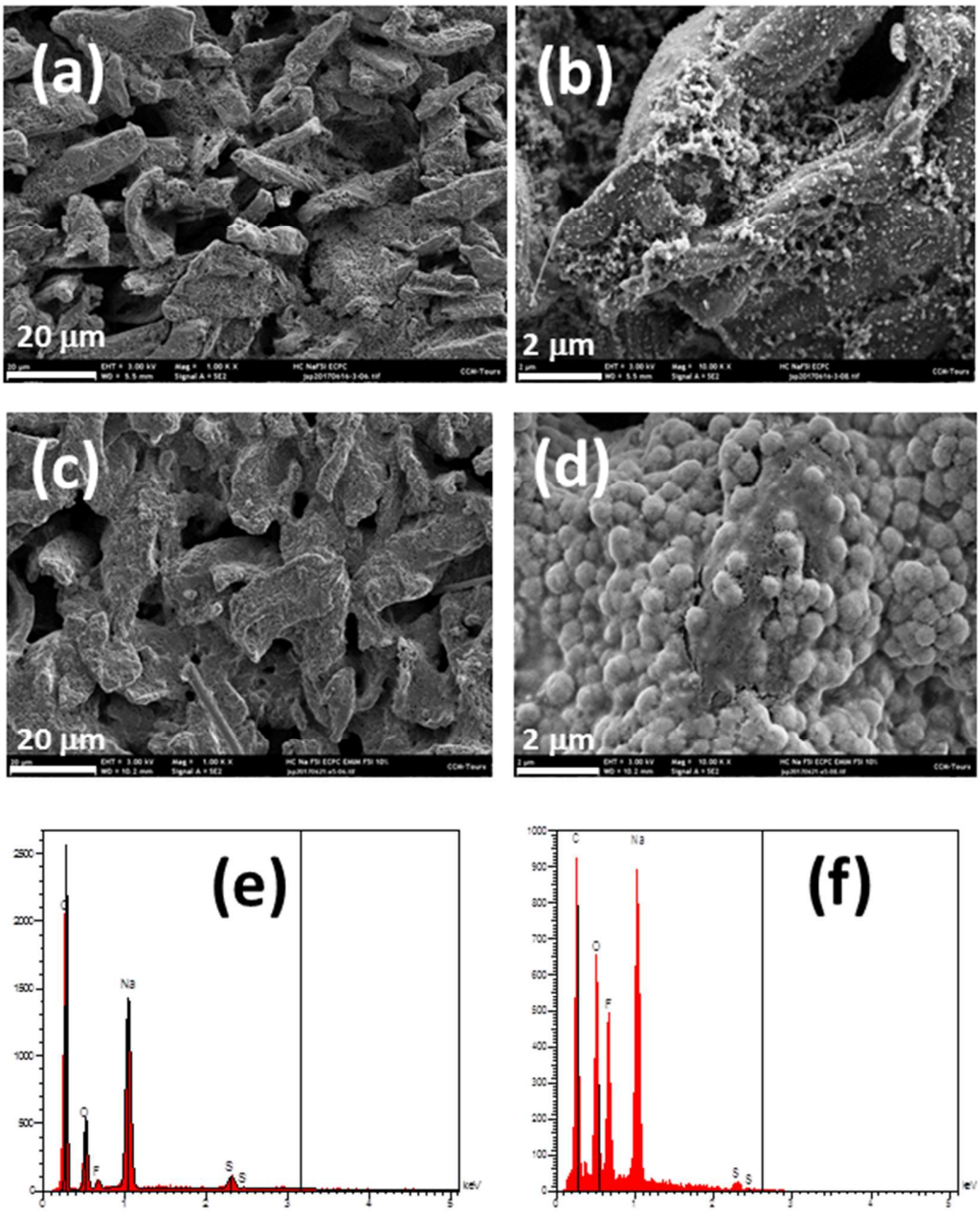

Figure 11: SEM micrographs of electrodes after 50 cycles in (a,b) 0%-EMImFSI and (c,d) 10%-EMImFSI NaFSI-based electrolytes at the discharged state. (e,f) Corresponding EDS mappings.

Coating particles formed in the 10%EMImFSI-NaFSI-cycled electrode (Figure 11d) are totally different to that found for 0%EMImFSI. They are submicronic sized and have a smooth ovoid shape. As for 10%EMImFSI-$NaPF_6$, EDS spectra (Figure 11f) indicate a large contribution of Na, O and F, and a lower amount of S from what expected from the FSI anion degradation. Thus, as for $NaPF_6$, one can consider that part of the degradation products are buried down to a NaF- and Na_2CO_3-rich film.

One of the SEI properties is its morphology, which has been analyzed and helps to understand the CE values. In resume, the presence of a true film protecting the hard carbon particles usually corresponds to stabilized interfaces that turn into CE constant values. This is the case of un-doped $NaClO_4$ and EMImFSI-doped $NaPF_6$ electrolytic solutions but is not evidenced for the NaFSI-based systems.

Another aspect of the SEI correlates to the extent of the capacity values that strongly depends on the chemical nature. For the $NaClO_4$, the SEI obtained for 10%EMImFSI-$NaClO_4$ was less stable than for EMImFSI-free system and presumably more resistive due to the presence of the S-containing compounds, resulting in -31% of capacity. The F-rich SEI observed in the EMImFSI-$NaPF_6$ combines a capacity increase of +50% from the EMImFSI-free electrolyte and stable CE values. Finally, the insoluble part of the SEI obtained for EMImFSI-NaFSI system, is also very rich in fluoride compounds but the capacity was 15% lower than with the EMImFSI, despite a better, but not constant CE. These results should be taken carefully and being contrasted with XPS measurements onto the cycled electrodes.

4. Conclusions

We have prepared nine electrolytes in order to determine the possible application of EMImFSI ionic liquid as additive (2% in weight ratio) or co-solvent (10% in weight ratio) for SIB r.t. electrolytes. From a physicochemical point of view, the introduction of EMImFSI implicates an ambiguous effect as ionic liquid adds ionic species to the solution but also enhances the viscosity. While the first factor governs the FSI– and PF_6–based electrolytes behavior, the second one rules the ClO_4-based electrolytes conductivity.

Sodium plating/stripping is very dependent on the sodium salt employed. For un-doped electrolytes, the extension of plating seems to be related to the dissociation degree of the sodium salt. EMImFSI introduction hinders systematically the plating for the $NaClO_4$- and $NaPF_6$-based electrolytes but increases it when present in 10% weight ratio for the NaFSI-based one. These features, rather than being related to the electrolytes viscosity, indicate that the SEI formed onto the collector involves the degradation of the ternary liquid mixture EMImFSI/EC/PC.

When a hard carbon electrode is submitted to slow CV in a sodium half-cell, one can distinguish several peaks associated to the reduction of FSI^- anion (as $EMIm^+$ is supposed to be stable from several reports) in the vicinity of 1.1V, 0.6V, 0.42V and 0.36V, depending on the EMImFSI content. Both, the FSI^- anion and electrolyte solvents degradation should provide a SEI on the hard carbon electrode and as a result, EMImFSI introduction penalizes the sodium storage in the hard carbon, even for the NaFSI-based electrolyte.

A different SEI is also responsible for a distinct polarization of the hard carbon electrodes after a deep discharge. In a general way, the polarization following the first discharge increases with the introduction of EMImFSI, which seems to be general when IL are present in electrolytic media. Nevertheless, after six cycles that consider switching from C/10 to C/5 regime, the polarization for 2%EMImFSI-based electrolytes is smaller or similar to that of un-doped ones. Only the charge/discharge curves associated to $NaPF_6$-containing electrolytes are different to the fingerprint curve of a hard carbon electrode, indicating active participation of EMImFSI in the capacity.

After six cycles, the highest capacities for each sodium salt series are 175 $mAh \cdot g^{-1}$ (for un-doped $NaClO_4$ electrolyte), 150 $mAh \cdot g^{-1}$ (for 2%EMImFSI/$NaPF_6$ electrolyte) and 179 $mAh \cdot g^{-1}$ (for un-doped NaFSI electrolyte). These values are to be compared with those obtained when classic FEC additive is introduced in the electrolyte formulation [175 $mAh \cdot g^{-1}$ (for $NaClO_4$ electrolyte), 134 $mAh \cdot g^{-1}$ (for $NaPF_6$ electrolyte) and 215 $mAh \cdot g^{-1}$ (for un-doped NaFSI electrolyte)]. Except for $NaPF_6$, the capacity retention is higher in FEC-doped than in un-doped or EMImFSI-doped electrolytes. In all the cases, the 2% EMImFSI content yields the lower retention values. This irregularity in the trend observation is confirmed after 25 galvanostatic cycles, where half-cells with FEC-doped electrolytes provide 55 or 90 $mAh \cdot g^{-1}$ more than $NaClO_4$ or NaFSI electrolyte, respectively, but -15 $mAh \cdot g^{-1}$ for $NaPF_6$ electrolyte.

CE is unstable in most of the electrolyte/electrodes systems analyzed in this work. There is not a marked trend except for FEC-doped, un-doped $NaClO_4$ and 10%EMImFSI-doped $NaPF_6$ electrolytes that give CE values with suitable stability and values in the 97.5-100% during 25 cycles. SEM observations indicate that this feature is ascribed to the absence of a suitable film efficiently recovering and connecting the hard carbon particles present in the electrode. Once this SEI has been formed, CE remains stable and capacity is efficiently retained.

The different features observed are unambiguously associated to the complexity of the SEI formed for each electrode/electrolyte combination as a result of the electrolyte components degradation. From EDS results, it is inferred that sodium salt decomposes in any case providing chlorine, fluorine and sulphur compounds for $NaClO_4$, $NaPF_6$ and NaFSI respectively, although the major SEI components are Na_2CO_3 from the EC/PC decomposition. FSI^- anion degradation yielding mainly sulphur is noticed when EMImFSI is doping the electrolyte. The exact chemical nature of the SEI should be checked in order to comprehend the cycling properties, as formation of resistive compounds should increase the electrode impedance, whereas major presence of ionic conductive compounds (mainly Na_2CO_3) account for cycling properties enhancement. XPS measurements will be relevant for clarify the SEI nature although one should be careful that washing with DMC we probably remove part of the SEI and we miss precious information on it.

From a technological point of view, we have demonstrated that, compared with FEC, EMImFSI is neither a suitable additive neither co-solvent for the r.t. SIB. Only in selected $NaPF_6$-based formulations, EMImFSI introduction represents a very low increase (9%) in the capacity provided by the hard carbon electrode referred to FEC addition in 2%. Unlike, capacities are below 150 $mAh \cdot g^{-1}$ for the rest of the EMImFSI-based formulations whereas FEC-based ones surpass 170 $mAh \cdot g^{-1}$. The above mentioned is not contradictory with the possible application of EMImFSI as sole solvent in the electrolyte (see the high capacity values that it can provide in combination with NaFSI). Accessorily, our study is also revealing the excellent properties of combining NaFSI as sodium salt and FEC as additive for r.t. SIB electrolytes.

Acknowledgement

This work was funded by the Région Centre through the ALBATTROS project (APR IA 2014 00094567) and Laboratoire de Recherche Correspondant CEA Le Ripault-PCM2E for a fellowship (MB). Authors would like to acknowledge Dr. Josefa Ortiz-Bustos (Departamento de Tecnología Química y Medio Ambiente, Universidad Rey Juan Carlos, Móstoles, Spain) and Pr. Encarnación Raimundo-Pineyro (CEMHTI, CNRS- Université d'Orléans, France) for recording and discussing the XRD patterns and BET measurements, respectively. Authors are also indebted to Dr. Pierre-Yvan Reynal for SEM measurements. Dr. Bénédicte Montigny, Gr. Barthélemy Aspe and Gr. Chalal Tchafouat (PCM2E) are acknowledged for providing hard carbon samples, additional electrochemical tests and helpful discussions.

References

1. Veronica Palomares, Paula Serras, Irune Villaluenga, Karina B. Hueso, Javier Carretero-Gonzàlez, Teófilo Rojo, *Na-ion batteries*, *Recent advances and present challenges to become low cost energy storage systems*, Ener. Env. Sci. 5 (2012) 5884.
2. Michael D. Slater, Donghan Kim, Eungje Lee, Christopher S. Johnson, *Sodium-ion batteries*, Adv. Funct. Mater. 23 (2013) 947.
3. Huilin Pan, Yong-Sheng Hu, Liquan Chen, *Room-temperature stationary sodium-ion batteries for large-scale electric energy storage*, Ener. Environ. Sci. 6 (2013) 2338.
4. Mouad Dahbi, Naoaki Yabuuchi, Kei Kubota, Kazuyasu Tokiwa, Shinichi Komaba, *Negative electrodes for Na-ion batteries*, Phys.Chem.Chem.Phys. 16 (2014) 15007.

5. Youngjin Kim, Kwang-Ho Ha, Seung M. Oh, Kyu Tae Lee, *High-Capacity anode materials for Sodium-ion batteries*, Chem. Eur. J. 20 (2014) 11980.
6. Xingde Xiang, Kai Zhang, Jun Chen, *Recent advances and prospects of cathode materials for Sodium-ion batteries*, Adv. Mater. 27 (2015) 5343.
7. Luyuan Paul Wang, Linghui Yu, Xin Wang, Madhavi Srinivasana, Zhichuan J. Xu, *Recent developments of electrode materials for sodium ion batteries*, J. Mater. Chem. A 3 (2015) 9353.
8. C. Nithya, S. Gopukumar, *Sodium ion batteries: a newer electrochemical storage*, WIREs Energy Environ 2015, 4, 253.
9. Monica Sawicki, Leon L. Shaw*, Advances and challenges of Sodium ion batteries as post Lithium ion batteries***,** RSC Advances 5 (2015) 53129.
10. Alexandre Ponrouch, Elena Marchante, Matthieu Courty, Jean-Marie Tarascon, M. Rosa Palacín, *In search of an optimized electrolyte for Na-ion batteries*, Energy Environ. Sci. 5 (2012) 8572.
11. Amrtha Bhide, Jonas Hofmann, Anna Katharina Dürr, Jürgen Janek, Philipp Adelhelm, *Electrochemical stability of non-aqueous electrolytes for sodium-ion batteries and their compatibility with* $Na_{0.7}CoO_2$, Phys.Chem.Chem.Phys. 16 (2014) 1987.
12. Gebrekidan Gebresilassie Eshetu, Sylvie Grugeon, Huikyong Kim, Sangsik Jeong, Liming Wu,Gregory Gachot, Stephane Laruelle, Michel Armand, Stefano Passerini, *Comprehensive insights into the reactivity of electrolytes based on Sodium ions*, ChemSusChem 9 (2016) 462.
13. A. Ponrouch, D. Monti, A. Boschin, B. Steen, P. Johansson, M. Rosa Palacín, *Non-aqueous electrolytes for sodium-ion batteries*. J. Mater. Chem. A 3 (2015) 22.

14. K. Vignarooban, R. Kushagra, A. Elango, P. Badami, B.-E. Mellander, X. Xu, T.G. Tucker, C. Nam, A.M. Kannan, *Current trends and future challenges of electrolytes for sodium-ion batteries*, Int. J. Hydrogen 41 (2016) 2829.
15. Haiying Che, Suli Chen, Yingying Xie, Hong Wang, Khalil Amine, Xiao-Zhen Liao, Zi-Feng Ma, *Electrolyte design strategies and research progress for room temperature sodium-ion batteries,* Energy Environ. Sci.10 (2017) 1075.
16. Guinevere A. Giffin, *Ionic liquid-based electrolytes for "beyond lithium" battery technologies*, J. Mater. Chem. A 4 (2016) 1337.
17. Clement Bommier, Xiulei Ji, *Electrolytes, SEI formation, and binders: A review of nonelectrode factors for Sodium-ion battery anodes*, Small 14 (2018) 1703576.
18. Shinichi Komaba, Wataru Murata, Toru Ishikawa, Naoaki Yabuuchi, Tomoaki Ozeki, Tetsuri Nakayama, Atsushi Ogata, Kazuma Gotoh, Kazuya Fujiwara, *Electrochemical Na insertion and solid electrolyte interphase for hard-carbon electrodes and application to Na-ion batteries*, Adv. Funct. Mater. 21 (2011) 3859.
19. P. Thomas, J. Ghanbaja, D. Billaud, *Electrochemical insertion of sodium in pitch-based carbon fibres in comparison with graphite in $NaClO_4$–ethylene carbonate electrolyte*, Electrochimica Acta 45 (1999) 423.
20. D. I. Iermakova, R. Dugas, M. R. Palacin, A. Ponrouch, *On the comparative stability of Li and Na metal anode interfaces in conventional alkyl carbonate electrolytes*, J. Electrochem. Soc. 162 (13) (2015) A7060.
21. Jun Yeong Jang, Hyungsub Kim, Yongwon Lee, Kyu Tae Lee, Kisuk Kang, Nam-Soon Choi, *Cyclic carbonate based-electrolytes enhancing the electrochemical performance of $Na_4Fe_3(PO_4)_2(P_2O_7)$ cathodes for sodium-ion batteries*, Electrochemistry Communications 44 (2014) 74.

22. E. Peled, S. Menkin, *Review-SEI: past, present and future,* Journal of The Electrochemical Society, 164 (7) (2017) A1703.
23. Hemant Kumar,Eric Detsi, Daniel P. Abraham, Vivek B. Shenoy, *Fundamental mechanisms of solvent decomposition involved in solid-electrolyte interphase formation in Sodium ion batteries*, Chem. Mater. 28 (2016) 8930.
24. Ronnie Mogensen, Daniel Brandell, Reza Younesi*, Solubility of the solid electrolyte interphase (SEI) in Sodium ion batteries*, ACS Energy Lett. 1 (2016) 1173.
25. Shinichi Komaba,Toru Ishikawa,Naoaki Yabuuchi,Wataru Murata, Atsushi Ito,Yasuhiko Ohsawa, *Fluorinated ethylene carbonate as electrolyte additive for rechargeable Na batteries*, ACS Appl. Mater. Interfaces 3 (2011) 4165.
26. Mouad Dahbi,Takeshi Nakano, Naoaki Yabuuchi, Shun Fujimura,Kuniko Chihara,Kei Kubota, Jin-Young Son, Yi-Tao Cui, Hiroshi Oji, Shinichi Komaba, *Effect of hexafluorophosphate and fluoroethylene carbonate on electrochemical performance and the surface layer of hard carbon for Sodium-ion batteries*, ChemElectroChem 3 (2016) 1856.
27. Kei Kubota, Shinichi Komaba, *Review-Practical issues and future perspective for Na-Ion batteries*, Journal of The Electrochem. Soc. 162 (14) (2015) A2538.
28. Mouad Dahbi, Mika Fukunishi, Tatsuo Horiba, Naoaki Yabuuchi, Satoshi Yasuno, Shinichi Komaba, *High performance red phosphorus electrode in ionic liquid-based electrolyte for Na-ion batteries*, J. Power Sourc. 363 (2017) 404.
29. Jun Yeong Jang, Yongwon Lee, Youngjin Kim, Jeongmin Lee, Sang-Min Lee, Kyu Tae Lee, Nam-Soon Choi*, Interfacial architectures based on a binary additive combination*

for high-performance Sn_4P_3 anodes in sodium-ion batteries, J. Mater. Chem. A 3 (2015) 8332.

30. A. Ponrouch, A.R. Goñi, M. Rosa Palacín, *High capacity hard carbon anodes for sodium ion batteries in additive free electrolyte*, Electrochem. Comm. 27 (2013) 85.
31. J. Serra Moreno, G.Maresca, S. Panero, B. Scrosati, G.B. Appetecchi, *Sodium-conducting ionic liquid-based electrolytes*, Electrochem. Comm. 43 (2014) 1.
32. Atsushi Fukunaga, Toshiyuki Nohira, Yu Kozawa, Rika Hagiwara, Shoichiro Sakaib, Koji Nitta, Shinji Inazawa, *Intermediate-temperature ionic liquid NaFSA-KFSA and its application to sodium secondary batteries*, J. Power Sourc. 209 (2012) 52.
33. Takayuki Yamamoto, Toshiyuki Nohira, Rika Hagiwara, Atsushi Fukunaga, Shoichiro Sakai,Koji Nitta, Shinji Inazawa, *Charge-discharge behavior of tin negative electrode for a sodium secondary battery using intermediate temperature ionic liquid sodium bis(fluorosulfonyl)amide-potassium bis(fluorosulfonyl)amide,* J. Power Sourc. 217 (2012) 479.
34. Changsheng Ding, Toshiyuki Nohira, Keisuke Kuroda, Rika Hagiwara, Atsushi Fukunaga, Shoichiro Sakai, Koji Nitta, Shinji Inazawa, *NaFSA-C1C3pyrFSA ionic liquids for sodium secondary battery operating over a wide temperature range*, J. Power Sourc. 238 (2013) 296.
35. Atsushi Fukunaga, Toshiyuki Nohira, Rika Hagiwara, Koma Numata, Eiko Itani, Shoichiro Sakai, Koji Nitta, Shinji Inazawa, *A safe and high-rate negative electrode for sodium-ion batteries: Hard carbon in NaFSA-C1C3pyrFSA ionic liquid at 363 K*, J. Power Sourc. 246 (2014) 387.

36. Kazuhiko Matsumoto, Takafumi Hosokawa, Toshiyuki Nohira, Rika Hagiwara, Atsushi Fukunaga, Koma Numata, Eiko Itani, Shoichiro Sakai, Koji Nitta, Shinji Inazawa, *The Na[FSA]-[C2C1im][FSA] (C2C1im$^+$:1-ethyl-3-methylimidazolium and FSA$^-$:bis(fluorosulfonyl)amide) ionic liquid electrolytes for sodium secondary batteries*, J. Power Sourc. 265 (2014) 36.
37. Changsheng Ding, Toshiyuki Nohira, Rika Hagiwara, Kazuhiko Matsumoto, Yu Okamoto, Atsushi Fukunaga, Shoichiro Sakai, Koji Nitta, Shinji Inazawa, *Na[FSA]-[C3C1pyrr][FSA] ionic liquids as electrolytes for sodium secondary batteries: Effects of Na ion concentration and operation temperature*, J. Power Sourc. 269 (2014) 124.
38. Kazuhiko Matsumoto, Yu Okamoto, Toshiyuki Nohira, Rika Hagiwara, *Thermal and Transport Properties of Na[N(SO$_2$F)$_2$]−[N-Methyl-N-propylpyrrolidinium][N(SO$_2$F)$_2$] Ionic Liquids for Na Secondary Batteries*, J. Phys. Chem. C 119 (2015) 7648.
39. Changsheng Ding, Toshiyuki Nohira, Atsushi Fukunaga, Rika Hagiwara, *Charge-discharge performance of an ionic liquid-based sodium secondary battery in a wide temperature range*, Electrochemistry 83(2) (2015) 91.
40. Atsushi Fukunaga, Toshiyuki Nohira, Rika Hagiwara, Koma Numata, Eiko Itani, Shoichiro Sakai, Koji Nitta, *Performance validation of sodium-ion batteries using an ionic liquid electrolyte,* J. Appl. Electrochem. 46 (2016) 487.
41. Changsheng Ding, Toshiyuki Nohira, Rika Hagiwara, *Electrochemical performance of Na$_2$Ti$_3$O$_7$/C negative electrode in ionic liquid electrolyte for sodium secondary batteries*, Journal of Power Sources 354 (2017) 10.

42. Rika Hagiwara, *Sodium ion batteries using ionic liquids*, in Electrochemical Science for a Sustainable Society, A tribute to John O'M Bockris, K. Ousaki Ed., Springer 2017, p. 197.

43. Siti Aminah Mohd Noor, Patrick C. Howlett, Douglas R. MacFarlane, Maria Forsyth, *Properties of sodium-based ionic liquid electrolytes for sodium secondary battery applications*, Electrochimica Acta 114 (2013) 766.

44. Hyungook Yoon, Haijin Zhu, Aziliz Hervault, Michel Armand, Douglas R. MacFarlane, Maria Forsyth, *Physicochemical properties of N-propyl-Nmethylpyrrolidinium bis(fluorosulfonyl)imide for sodium metal battery applications*, Phys. Chem. Chem. Phys. 16 (2014) 12350.

45. Maria Forsyth, Hyungook Yoon, Fangfang Chen, Haijin Zhu, Douglas R. MacFarlane, Michel Armand, Patrick C. Howlett, *Novel Na^+ ion diffusion mechanism in mixed organic−inorganic ionic liquid electrolyte leading to high Na^+ transference number and stable, high rate electrochemical cycling of sodium cells*, J. Phys. Chem. C 120 (2016) 4276.

46. S.A.M. Noor, N.C. Su, L.T. Khoon, N.S. Mohamed, A. Ahmad, M.Z.A. Yahya, H. Zhu, M. Forsyth, D.R. MacFarlane, *Properties of high Na-ion content N-propyl-N-methylpyrrolidinium bis(fluorosulfonyl)imide-ethylene carbonate electrolytes*, Electrochimica Acta 247 (2017) 983.

47. Matthias Hilder, Patrick C. Howlett, Damien Saurel, Elena Gonzalo, Michel Armand, Teófilo Rojo, Douglas R. Macfarlane, Maria Forsyth, *Small quaternary alkyl phosphonium bis(fluorosulfonyl)imide ionic liquid electrolytes for sodium-ion batteries with P2- and O3-$Na_{2/3}[Fe_{2/3}Mn_{1/3}]O_2$ cathode material*, J. Power Sourc. 349 (2017) 45.

48. Nithinai Wongittharom, Chueh-Han Wang, Yi-Chen Wang, Cheng-Hsien Yang, Jeng-Kuei Chang, *Ionic liquid electrolytes with various sodium solutes for rechargeable Na/$NaFePO_4$ batteries operated at elevated temperatures*, ACS Appl. Mater. Interfaces 6 (2014) 17564.

49. Chueh-Han Wang, Yu-Wen Yeh, Nithinai Wongittharom, Yi-Chen Wang, Chung-Jen Tseng, Sheng-Wei Lee, Wen-Sheng Chang, Jeng-Kuei Chang, *Rechargeable Na/$Na_{0.44}MnO_2$ cells with ionic liquid electrolytes containing various sodium solutes*, J. Power Sourc. 274 (2015) 1016.

50. Chueh-Han Wang,Cheng-Hsien Yang,Jeng-Kuei Chang, *Suitability of ionic liquid electrolytes for room temperature sodium-ion battery applications*, Chem. Commun. 52 (2016) 10890.

51. Damien Monti, Erlendur Jónsson, M. Rosa Palacín, Patrik Johansson, *Ionic liquid based electrolytes for sodium-ion batteries: Na^+ solvation and ionic conductivity*, J. Power Sourc. 245 (2014) 630.

52. Damien Monti, Alexandre Ponrouch, M. Rosa Palacín, Patrik Johansson, *Towards safer sodium-ion batteries via organic solvent/ionic liquid based hybrid electrolytes*, J. Power Sourc. 324 (2016) 712.

53. Gurpreet Singh, Frederic Aguesse, Laida Otaegui, Eider Goikolea, Elena Gonzalo, Julie Segalini, Teofilo Rojo, *Electrochemical performance of $NaFe_x(Ni_{0.5}Ti_{0.5})_{1-x}O_2$ (x= 0.2 and x=0.4) cathode for sodium-ion battery*, J. Power Sourc. 273 (2015) 333.

54. Laida Otaegui, Eider Goikolea, Frederic Aguesse, Michel Armand, Teófilo Rojo, Gurpreet Singh, *Effect of the electrolytic solvent and temperature on aluminium current collector stability: A case of sodium-ion battery cathode*, J. Power Sourc. 297 (2015) 168.

55. Luciana Gomes Chagas, Daniel Buchholz, Liming Wu, Britta Vortmann, Stefano Passerini, *Unexpected performance of layered sodium-ion cathode material in ionic liquid-based electrolyte*, J. Power Sourc. 247 (2014) 377.
56. Ivana Hasa, Stefano Passerini, Jusef Hassoun, *Characteristics of an ionic liquid electrolyte for sodium-ion batteries*, Journal of Power Sources 303 (2016) 203.
57. Feng Wu, Na Zhu, Ying Bai, Libin Liu, Hang Zhou, Chuan Wu, *Highly safe ionic liquid electrolytes for Sodium-ion battery: wide electrochemical window and good thermal stability*, ACS Appl. Mater. Interfaces 8 (2016) 21381.
58. Ilya A. Shkrob, Timothy W. Marin, Ye Zhu, Daniel P. Abraham, *Why bis(fluorosulfonyl)imide is a "magic anion" for electrochemistry*, J. Phys. Chem. C 118 (2014) 19661.
59. Daniela Molina Piper, Tyler Evans, Kevin Leung, Tylan Watkins, Jarred Olson, Seul Cham Kim, Sang Sub Han, Vinay Bhat, Kuy Hwan Oh, Daniel A. Buttry, Se-Hee Lee, *Stable silicon-ionic liquid interface for next-generation lithium ion batteries*, Nature Comm. 6 (2015) 6230.
60. Akin Budi,Andrew Basile,George Opletal,Anthony F. Hollenkamp,Adam S. Best,Robert J. Rees,Anand I. Bhatt,Anthony P. O'Mullane, Salvy P. Russo, *Study of the initial stage of solid electrolyte interphase formation upon chemical reaction of lithium metal and N-methyl-N-propyl-pyrrolidinium-bis(fluorosulfonyl)imide*, J. Phys. Chem. C 116 (2012) 19789.

61. Simon Sayah, Fouad Ghamouss, François Tran-Van, Jesús Santos-Peña, Daniel Lemordant, *A bis(fluorosulfonyl)imide based ionic liquid as safe and efficient electrolyte for Si/Sn-Ni/C/Al composite anode*, Electrochimica Acta 243 (2017) 197.
62. Masashi Ishikawa, Toshinori Sugimoto, Manabu Kikuta, Eriko Ishiko, Michiyuki Kono, *Pure ionic liquid electrolytes compatible with a graphitized carbon negative electrode in rechargeable lithium-ion batteries*, J. Power Sourc. 162 (2006) 658.
63. P. Vogel, Phys. Z. 22 (1921) 645.
64. G. Tamman, W. Hesse, *Die abhangigkeit der viscositat von der temperatur bei unterkühlten Flüssigkeiten*, Z. Anorg. Allg. Chem. 156 (1926) 245.
65. G.S. Fulcher, *Analysis of recent mesures of the viscosity of glasses*, J. Am. Ceram. Soc. 8 (1925) 339.
66. R. Richert, C. A. Angell, *Dynamics of glass-forming liquids. V. On the link between molecular dynamics and configurational entropy,* The Journal of Chemical Physics 108 (21) (1998) 9016.
67. Jagabandhu Patra, Hao-Tzu Huang, Weijiang Xue, Chao Wang, Ahmed S. Helal, Ju Li, Jeng-Kuei Chang, *Moderately concentrated electrolyte improves solid-electrolyte interphase and sodium storage performance of hard carbon*, Energy Storage Materials 16 (2019) 146.
68. Yan Zhang, Aditya Narayanan, Frieder Mugele, Martien A. Cohen Stuart, Michel H.G. Duits, *Charge inversion and colloidal stability of carbon black in battery electrolyte solutions*, Colloids and Surfaces A: Physicochem. Eng. Aspects 489 (2016) 461.
69. Matthias Schmeisser, Peter Illner, Ralph Puchta, Achim Zahl, Rudi van Eldik, *Gutmann donor and acceptor numbers for ionic liquids*, Chem. Eur. J. 18 (2012) 10969.

70. P. A. Brooksby, W. R. Fawcett, *Infrared (attenuated total reflection) study of propylene carbonate solutions containing lithium and sodium perchlorate*, Spectrochimica Acta Part A 64 (2006) 372.

71. D. S. Tchitchekova, D. Monti, P. Johansson, F. Bardé, A. Randon-Vitanova, M. R. Palacín, A. Ponrouch, *On the reliability of half-cell tests for monovalent (Li^+, Na^+) and divalent (Mg^{2+}, Ca^{2+}) cation based batteries*, Journal of The Electrochemical Society, 164 (7) (2017) A1384.

72. D.A. Stevens, J. R. Dahn, *The mechanisms of lithium and sodium insertion in carbon materials*, J. Electrochem. Soc. 148 (8) (2001) A803.

73. Clément Bommmier, Todd Wesley Surta, Michelle Dogos, Xiulei Ji, *New mechanistic insights on Na-ion storage in non-graphitizable carbon*, Nano Letters 15 (2015) 5888.

74. Hongshuai Hou, Xiaoqing Qiu, Weifeng Wei, Yun Zhang, Xiaobo Ji, *Carbon anode materials for advanced Sodium-ion batteries*, Adv. Energy Mater. 7 (2017) 1602898.

75. V. A. Oltean, B. Philippe, S. Renault, R. Felix Duarte, H. Rensmo, D. Brandell, *Investigating the interfacial chemistry of organic electrodes in Li and Na-Ion batteries*, Chem. Mater. 28 (2016) 8742.

76. Yue Pan, Yuzi Zhang, Bharathy S. Parimalam, Cao Cuong Nguyen, Guiling Wang, Brett L. Lucht, *Investigation of the solid electrolyte interphase on hard carbon electrode for sodium ion batteries*, Journal of Electroanalytical Chemistry 799 (2017) 181.

77. T. Vogl, C. Vaalma, D. Buchholz,M. Secchiaroli, R. Marassi, S. Passerini, A. Balducci, *The use of protic ionic liquids with cathodes for sodium-ion batteries*, J. Mater. Chem. A 4 (2016) 10472.

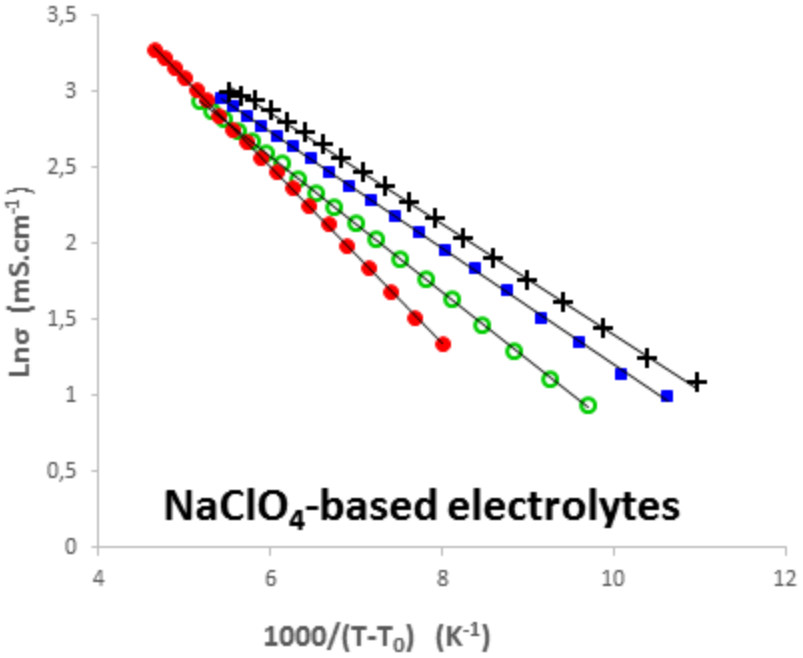
Lnσ (mS.cm-1)
1000/(T-T0) (K-1)
NaClO4-based electrolytes

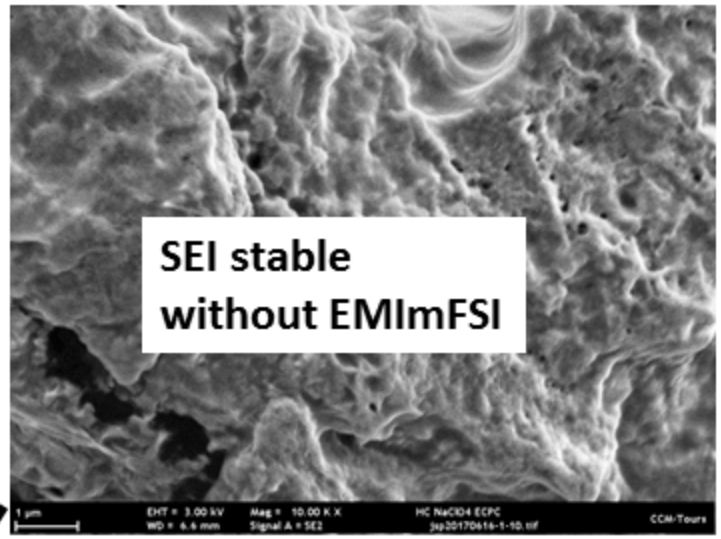
SEI stable
without EMImFSI

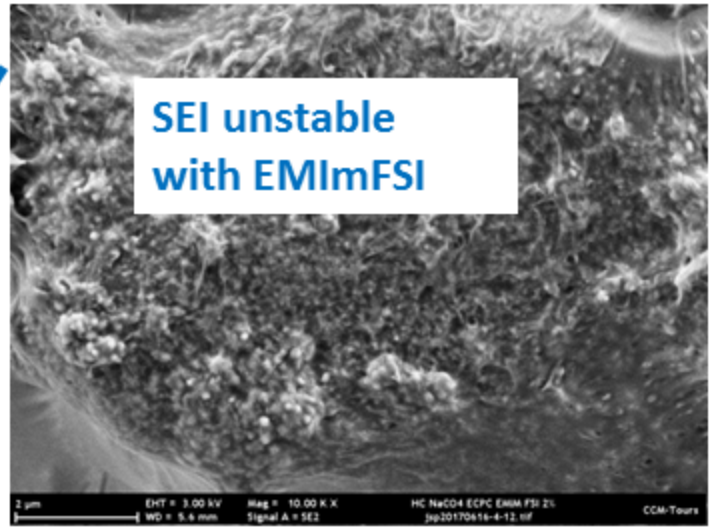
SEI unstable
with EMImFSI

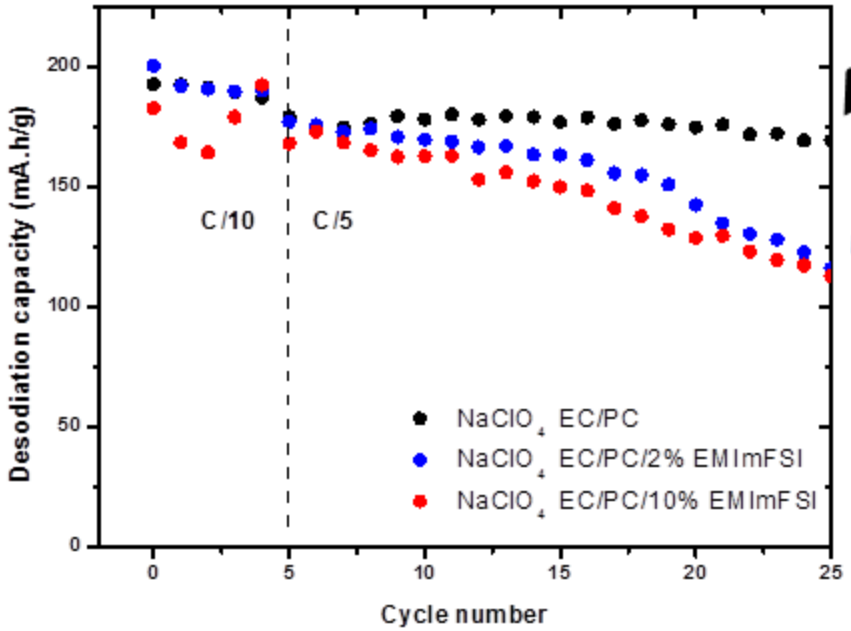
Desodiation capacity (mA.h/g)
Cycle number
C/10
C/5
NaClO4 EC/PC
NaClO4 EC/PC/2% EMImFSI
NaClO4 EC/PC/10% EMImFSI